Naval Oceanographic and
Atmospheric Research Laboratory

Technical Note 83
October 1990

Environmental Conditions in the Gulf of Mexico During November-December

J. D. Boyd
Oceanography Division
Ocean Science Directorate

L. A. Jugan
M. A. Rich
B. J. Roser
Planning Systems Incorporated
Slidell, Louisiana

These working papers were prepared for the timely dissemination of information; this document does not represent the official position of NOARL.

Abstract

Environmental information for the Gulf of Mexico was analyzed in support of an upcoming experiment. Available oceanographic, meteorological, and geological properties of the Gulf, with specific emphasis on the area between 24-29°N and 90-95°W, are summarized for the November-December time frame.

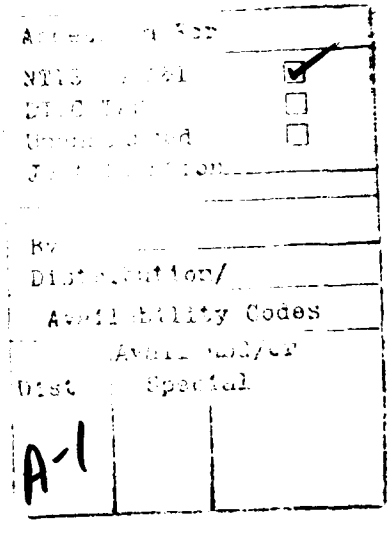

Acknowledgments

We wish to thank those who assisted in the processing of data used to compile this technical note: J.W. Cartmill of Planning Systems Incorporated and R.S. Linzell of Neptune Technologies. R.L. Crout of Planning Systems assisted in the review and clarification of Loop Current and eddy formation processes.

This technical note was sponsored by the Office of Naval Technology (ONT) through the Naval Oceanographic and Atmospheric Research Laboratory (NOARL), Ocean Acoustics and Technology Directorate, M. Fagot, Program Manager, under Program Element 62435N.

Contents

ENVIRONMENTAL CONDITIONS IN THE GULF OF MEXICO DURING NOVEMBER-DECEMBER

1.0 Introduction

The purpose of this technical note is to describe some of the environmental conditions in a region of the Gulf of Mexico in which an experiment will take place in November and December 1990. The general area of interest lies between 24-29°N and 90-95°W, as illustrated in Figure 1-1. The experiment location will be at or near 26°40'N, 92°30'W. This note provides a review of the oceanographic and meteorological variables that may affect acoustic properties and deployed instrumentation during this experiment. Oceanographic and atmospheric characteristics for the area are presented, with specific emphasis on the conditions during November and December.

2.0 Oceanography

2.1 Water Column

Temperature and Salinity. Temperature and salinity values for the Gulf of Mexico during the months of November and December were extracted from the Master Oceanographic Observation Data Set (MOODS). The station locations for which MOODS data are available in the Gulf are shown in Figure 2-1. A subset of this, within the box indicated on Figure 2-1, was examined to determine expected conditions near the experiment site. The profiles from the locations within the box are plotted in Figures 2-2 and 2-3. From these profiles, the most commonly occurring (mode) temperature and salinity values were chosen at individual depths, and the results are presented in Figure 2-4. These can be considered typical temperature and salinity profiles for the study region.

In addition, climatological temperature and salinity data were extracted from the Generalized Digital Environmental Model (GDEM) for autumn at the experiment site. These temperature and salinity profiles are shown in Figure 2-5.

The profiles in Figures 2-4 and 2-5 are fairly consistent in their structure. The surface layer is fairly well mixed to about 75 m or so, with a temperature of 23°C and a salinity of 36.3 ppt. Temperature decreases steadily below 75 m, reaching 9°C at 500 m. Temperature still decreases below this, but not as rapidly and reaches 5°C at 1000 m. Below 1000 m, the temperature is fairly constant at 4.3°C. Salinity is a steady 36.3 in the upper layer of the water column; however, the salinity maximum occurs between 75 and 150 m, at 36.4 to 36.8 ppt. Salinity decreases steadily to a depth of 500 m and stabilizes between 34.8 and 34.9 below 500 m.

Figures 2-2 and 2-3 indicate that there is a good deal of variability in both temperature and salinity in the area of interest. This results from a number of factors, including the occasional occurrence of cold, fresh water from the Texas shelf in

the area; storm activity; and general variations in Loop Current/eddy activity (Nowlin and McLellan, 1967). Therefore, these "typical" values (and their associated sound speed profiles) should be used with caution.

Sound Speed. Table 2-1 lists the temperature and salinity values from the "typical" profiles of Figure 2-4 and includes calculated sound speed. Sound speed values were calculated using both the Chen and Millero equation (Fofonoff and Millard, 1983) and the DelGrosso (1973) equation. Corresponding plots of the sound speed profiles are presented in Figure 2-6.

Table 2-1. Typical temperature and salinity profiles corresponding to the plots in Figure 2-4 and associated sound speed profiles.

Depth (m)	Temperature (°C)	Salinity (ppt)	Sound Speed Chen/Millero ($m\ s^{-1}$)	Sound Speed DelGrosso ($m\ s^{-1}$)
0	23.04	36.36	1531.02	1530.98
10	23.05	36.37	1531.23	1531.18
20	23.05	36.37	1531.40	1531.34
50	23.05	36.37	1531.90	1531.83
76	20.30	36.46	1525.20	1525.14
100	18.82	36.43	1521.44	1521.39
126	17.87	36.41	1519.11	1519.07
150	16.91	36.28	1516.53	1516.48
200	15.26	36.01	1512.00	1511.95
250	13.73	35.77	1507.66	1507.61
300	12.41	35.55	1503.86	1503.79
350	11.20	35.37	1500.33	1500.25
400	10.33	35.24	1497.94	1497.84
450	9.56	35.13	1495.87	1495.76
500	8.89	35.05	1494.15	1494.02
550	8.09	34.96	1491.89	1491.73
600	7.46	34.91	1490.27	1490.09
650	6.88	34.88	1488.83	1488.63
700	6.46	34.88	1488.02	1487.81
750	6.00	34.89	1487.05	1486.82
800	5.70	34.90	1486.70	1486.46
850	5.51	34.90	1486.78	1486.52
900	5.38	34.91	1487.11	1486.83
950	5.23	34.92	1487.35	1487.06
1000	5.12	34.93	1487.75	1487.45
1200	4.50	34.93	1488.58	1488.23
1575	4.23	34.92	1493.79	1493.36
1750	4.18	34.90	1496.52	1496.07
1800	4.08	34.90	1496.96	1496.49

In addition, sound speeds calculated from the GDEM profiles in Figure 2-5 are plotted in Figure 2-7.

The figures illustrate that the sound speed profile decreases with depth to approximately 850 m, the location of the sound channel axis. Below 850 m the sound speed steadily increases. The sonic layer depth coincides with the depth of the mixed layer (75 m).

Temperature - Salinity Relationships. The temperature-salinity relationships for the MOODS and GDEM data (over the entire area of interest, see box in Figure 2-1) are shown in Figures 2-8 and 2-9.

The higher salinity values (36.6-36.7 ppt) are characteristic of Subtropical Underwater (Hofmann and Worley, 1986). This water mass is commonly centered around the 200 m depth. Below this, and extending to 800 or 1000 m, Antarctic Intermediate Water is seen as a low-salinity (34.8 ppt) water mass. Both Subtropical Underwater and Antarctic Intermediate Water are found in the Caymen Sea and are assumed to enter the Gulf through the Yucatan Strait (Nowlin and McLellan, 1967). In waters below 1000 m, North Atlantic Deep Water is present; waters are typically isohaline at 34.97 ppt (Hofmann and Worley, 1986). This water is assumed to enter the Gulf over the Yucatan sill (Nowlin and McLellan, 1967).

Mixed Layer Properties. In November and December, the mixed layer is generally found at depths between 75 and 100 m (Nowlin and McLellan, 1967). This has been found to be consistent for most studies (Hofmann and Worley, 1986; MMS, 1987), except when strong freshwater flow from the Texas shelf enters the area. This is rare, but when it occurs, a lens of cold, fresh water forms over warmer, more saline Gulf waters. Under these conditions, the mixed layer is reduced to a depth of 20 to 30 m.

The mixed layer is usually characterized by temperatures between 20 and 22°C and salinities between 36.2 and 36.4 ppt. Below the mixed layer, there is a steady decrease in both temperature and salinity to a depth of 1000 m. Below this, temperature and salinity vary little with depth.

2.2 Currents

General Circulation. Circulation in the Gulf of Mexico is dominated by two major features, an anticyclonic gyre in the west and the Loop Current in the east. This divides the Gulf into western and eastern provinces, as illustrated in Figure 2-10.

The gyre in the western Gulf is considered "quasi-permanent" (Behringer et al., 1977), since it always exists but its position within the Gulf varies with atmospheric and oceanographic conditions. The anticyclonic gyre in the western Gulf is driven by differential wind stress over the Gulf of Mexico. Eddies shed by the Loop Current complicate the flow, as illustrated by the numerical simulations in Figures 2-11 and 2-12 (Wallcroft, 1984). Figure 2-11 can be considered representative of Gulf circulation during winter and Figure 2-12 representative of the summer circulation, although the temporal variation in the Loop Current

intrusion into the Gulf causes significant changes in these patterns.

The anticyclonic flow of the gyre has been observed to depths of 3000 m (Smith, 1986). Surface current speeds up to 70 cm s^{-1} have been measured; however, the average speed is 7 to 14 cm s^{-1}. Maximum speeds are usually a result of strong winds associated with winter storms. Currents decrease to a speed of 1 to 18 cm s^{-1} at a depth of 1650 m, and average 2 cm s^{-1} near the bottom in deep water.

Loop Current. The Loop Current enters the Gulf of Mexico through the Yucatan Strait, extends into the eastern Gulf, then exits through the Florida Straits. The extent that the Loop Current penetrates into the Gulf is temporally and spatially variable. Behringer et al. (1977) suggest an 8 to 17 month cycle for Loop Current development and recession. In the early stages of this cycle, the Loop Current enters the Gulf of Mexico and immediately exits. In response to atmospheric forcing, the current penetrates farther into the Gulf. After reaching its maximum extent, the current then recedes. Behringer et al. (1977) postulated an average 1-year cycle based on a study of 4 separate data sets over 4 different years. Their results, based on a composite derived from the 4 years of data, are shown in Figure 2-13. Note that minimum penetration typically occurs in December through January (see Figure 2-14). Studies by Sturges and Evans (1983) estimate the maximum northern penetration into the Gulf occurs in August. Their annual pattern of the Loop Current's penetration and recession is shown in Figure 2-15.

The extent of penetration into the Gulf also varies from year to year. The average position of the Loop Current boundary at its maximum northern extent is approximately 27°30'N, as shown in Figure 2-16. Variations in the boundaries of the Loop Current have been studied by Minerals Management Service (MMS) (1986) and Sturges and Evans (1983). Figure 2-17 shows the variation in the east-west boundaries of the current between 25° and 27°N. Figure 2-18 presents the variation of the northern boundary over a 13-year period.

Currents associated with the Loop Current can exceed 200 cm s^{-1} in surface waters (Nowlin and McLellan, 1967). Such strong currents are more common when the Loop Current reaches the central Gulf, around 24°-25°N. Strongest speeds are associated with the "core" or western boundary of the current. When the current extends farther north in the Gulf, maximum speeds are approximately 70 cm s^{-1} (at 27°N). Strong currents extend to a depth of 100 m, but effects of the current are observed to depths of 450 m (Science Applications International Corporation, SAIC, 1989). However, associated loop current eddies, discussed below, can influence currents to a depth of 1600 m (Hamilton, 1990). In the absence of the Loop Current, surface current speeds are typically between 5 and 15 cm s^{-1}, with a maximum of 25 cm s^{-1} (Hofmann and Worley, 1986).

Both horizontal and vertical current shear is assumed to occur near the boundary of the Loop Current (MMS, 1987); however, there have been no studies attempting to quantify this.

Loop Current Eddies. Eddies generally form when the Loop Current reaches its northernmost position. Although it will vary from year to year, the mean location of the current when an eddy is shed is 25.5°N, 87.5°W (SAIC, 1989). Once separated, the eddy generally translates toward the west across the Gulf at speeds typically around 4-5 km d^{-1} (Elliot, 1982). The SAIC (1989) study indicates that a good majority of eddies observed during a 5-year period stalled at some point during their life span. The movement of an eddy as tracked by Elliot (1982) is shown in Figures 2-19a through 2-19c. The frequency distribution of translation speed is given in Figure 2-20.

The eddies have an anticyclonic motion, with a diameter of 150 to 400 km (Vukovich, 1988). (This is a characteristic distinguishing eddies from the western Gulf gyre, which has a diameter of nearly 1000 km.) Eddies generally retain their circulation pattern as they translate across the Gulf. Initially, eddies affect circulation in the upper 450 m of the water column; however, as they translate across the Gulf, the depth of their influence increases to a maximum of 1600 m (Hamilton, 1990). Typical paths of eddies are shown in Figure 2-21. In most years, one eddy is formed; however, up to four have been observed at one time (Elliot, 1982).

As an eddy translates across the Gulf, it may coalesce with another eddy. When this occurs, up to 20 percent of the water is ejected. For an anticyclonic eddy, this ejection of water causes "tails" at the top right and bottom left of the area of coalescence. This is shown in Figure 2-22. When this water interacts with Gulf waters, the result is usually a small, cyclonic eddy. When two eddies coalesce, the diameter of the resultant eddy is typically only 25 percent larger than the larger parent eddy (SAIC, 1989). Eddy decay is evidenced by the gradual shrinking diameter and can be caused by such factors as vertical mixing and heat loss to the atmosphere (Elliot, 1982), or atmospheric influences, topography, interaction with other strong flows and eddy-eddy interaction (Smith, 1986). The time from eddy formation to complete decay ranges from 6 to 15 months, with an average of 8 months (SAIC, 1989). Secondary eddies may be formed when two eddies interact or as a result of bottom interaction.

Surface current speeds associated with Loop Current eddies average 20 cm s^{-1}, but have been observed to be as strong as 92 cm s^{-1} (Forrestall, 1990). Currents stronger than 75 cm s^{-1} generally last less than 1 day. The strongest currents are usually found at the northern boundary of the eddy, with reduced current speeds at the southern boundary (one observation indicated an order of magnitude difference, 10 cm s^{-1} versus 100 cm s^{-1}, MMS, 1986).

Currents near the Experiment Site. Currents near 26°40'N, 92°30'W are generally less than 10 cm s^{-1} at all depths. This is

shown in Figure 2-23. (While Figure 2-23 gives geostrophic currents only, a nearby current meter mooring (SAIC, 1989) indicated that these values were representative of the complete current field.) These values are listed in Table 2-2. Currents in the upper 800 m of the water column tend to flow toward the east as part of the western Gulf gyre. Below 800 m, current flow is typically toward the west. These conditions may be considered typical for late November and the month of December.

Table 2-2. Average current speeds at the experiment site determined from contours in Hofmann and Worley (1986).

Depth (m)	Current Speed (cm s^{-1})	Direction (toward)
0 - 200	5 - 10	E
100 - 700	0 - 5	E
700 - bottom	0 - 5	W

Although the Loop Current rarely reaches the experiment site, if Loop Current eddies are in the immediate experiment area, current speeds will increase significantly. SAIC (1989) conducted an 18-month study of currents at a station near the experiment site (26° 44.4'N, 90° 59.7'W). Maximum speeds at various depths at this station are listed in Table 2-3.

Table 2-3. Maximum current speed and associated direction based on observed values obtained from Forrestall (1990) (surface value) and SAIC (1989) (values at depth) for a location near the experiment site during the occurrence of an eddy.

Depth (m)	Current Speed (cm s^{-1})	Direction (toward)
0	92	-
100	82	142°
300	44	136°
725	23	145°
1650	14	123°

It should be noted that these measurements in Table 2-3 were taken during the summer (August) and that there have been no data obtained in winter during those rare instances when the Loop Current has penetrated as far north as the experiment site. Current directions will vary significantly depending on whether the Loop Current extends into the area or if an eddy is moving through.

Severe winter storms may also affect surface currents at the experiment site. Surface current speeds can be expected to exceed 25 cm s^{-1} during winter storms (MMS, 1984). Associated winds from

the north force currents to flow to the south temporarily.

2.3 Topographic Rossby Waves.

Velocity fluctuations (of up to 2 cm s^{-1}) observed by Hamilton (1990) have been identified as topographic Rossby waves (TRWs). It is postulated that they are caused by Loop Current interaction with the west Florida continental shelf. TRW's travel westward across the Gulf of Mexico at translation speeds of approximately 9 km d^{-1} (as opposed to the 3 to 6 km d^{-1} translation speeds typical of Loop Current eddies). Spectral peaks occur at periods equal to 25 days and 40 to 100 days. TRW wavelengths range from 150 to 220 km in the high frequency band and 120-300 km in the low frequency band.

2.4 Surface Waves

In the area during November and December, available wave height observations (the average of wave height and direction taken over the time frame allotted for the observation, with "wave height" presumably being significant wave height) prior to 1975 indicate that surface waves are less than 2 m in height nearly 80 percent of the time (Defense Mapping Agency, 1976). This is because of the relatively weak winds during these months (refer to Section 3.2). Waves greater than 2 m occur 20 percent of the time, as shown in Figure 2-24. Waves between 2 and 4 m in height are usually the result of strong winds occurring during winter storms and passing cold fronts.

Waves are typically from the eastern quadrant, with 25 percent coming directly from the east. Waves as high as 8 m have been observed in this area; however, this observation was made during the only recorded tropical storm to enter this area over a 100-year period (Naval Oceanography Command Detachment, 1986).

2.5 Summary

During a typical November and December, oceanographic conditions at the experiment site are fairly calm. The water column structure is generally predictable but can be affected by the intrusion of fresher, colder water from the coast. The mixed layer extends to a depth typically between 75 and 100 m and the sound channel axis is located around 850 m. Currents are generally less than 10 cm s^{-1} (Hofmann and Worley, 1986).

Conditions near the experiment site when the Loop Current extends into the area (rare during November and December) or when an eddy is present (a more common occurrence) are more energetic. Water column structure is disrupted and currents reaching 92 cm s^{-1} at the surface have been observed. The effects of the Loop Current have been observed to a depth of 450 m; however, the effects of eddies have been observed to a depth of 1600 m (Hamilton, 1990).

Velocity fluctuations up to 2 cm s^{-1} are caused by topographic Rossby waves that are assumed to be caused by the interaction of

the Loop Current with the continental shelf (Hamilton, 1990). Surface waves in November and December are typically less than 3 m and are from the eastern quadrant. Waves greater than 4 m can result from strong winds associated with winter storms and passing cold fronts.

3.0 Meteorology

3.1 General Circulation

The general circulation over the Gulf of Mexico is dominated by the Bermuda High, which is centered over the northwestern Atlantic Ocean. Flow along the southern domain of this High produces the large scale northeastern flow known as the trade winds. During winter, the High is weakest and at its eastern-most position, causing a weakening of the easterly trade winds and thereby producing the weakest trade wind flow of the year (Naval Oceanography Command Detachment, 1986). The weakening of the Bermuda High allows cold air from the continental U.S. (cold frontal passage) to move into the Gulf of Mexico to produce northwesterly winds and increasing cloud cover, and causing lower temperatures. Generally, cold fronts are modified by the tropical conditions of the Gulf of Mexico; therefore, the occurrence of winter storms is rare at the experiment site. Cold fronts enter the area every 7 to 10 days on average, and affect the area for a duration of less than 2 days. In the area of interest, winter is a dry season with partly cloudy skies, with predominantly light winds from the east.

3.2 Winds

Generally, the Gulf of Mexico is under the influence of easterly trade winds that range in speed from 11 to 17 kt (Meserve, 1974). The distribution of wind speed and direction is given in Figure 3-1. When winter cold fronts move into the Gulf of Mexico, winds are from the northwest at speeds up to 20 kt. Gale force winds (in excess of 34 kt) are rare, but have been observed. Thunderstorms along the boundaries of cold fronts can produce gusty winds to 30 kt and periods of heavy precipitation.

3.3 Storms

Winter storms are not common in this area; however, passing cold fronts may have associated thunderstorms along their boundaries. Cold fronts are quickly modified by the tropical climate of the Gulf region and the severity and occurrence of thunderstorms are significantly reduced in the area of interest. From November-December 1886 to November-December 1986, there was one recorded tropical storm within 120 nmi of the area of interest (Neumann et al., 1987). The typical track of fronts entering the area is shown in Figure 3-2. Note that as cold fronts from the north enter the Gulf, cold air mixes with maritime tropical air This causes the stationary front seen in Figure 3-2. This front generally lasts 2-4 days and is accompanied by slow, steady rain.

Cold fronts, with associated storms and rain, rarely reach the experiment area.

3.4 Cloud Cover

Clouds tops seldom extend higher than 3,000 to 5,000 ft because of the trade wind inversion which occurs between these levels (Naval Oceanography Command Detachment, 1986). During winter, sky conditions vary between partly cloudy to mostly cloudy. Cumulus and stratocumulus clouds are the most common types of clouds encountered. Cloud base is usually 2,000 ft; however, during frontal passage the cloud base is lowered to 1,000 ft.

3.5 Summary

Meteorological conditions near the experiment site are generally calm during November and December. Occasionally, winter storms and passing cold fronts may bring winds reaching 30 kt, waves reaching 4 m, mostly cloudy skies, and precipitation. Tropical storms are not common in the area during November and December, and only one tropical storm has been recorded in the area during these months over a 100-year period.

4.0 Shipping Traffic and Other Activities

The experiment site is located at the southerly edge of offshore drilling and pipeline activity (MMS, 1983). However, most of the shipping traffic is to the north of the experiment site. In addition, there are military warning areas to the east and west of the experiment site. During use, these areas are sites of carrier maneuvers, missile testing, rocket firing, pilot training, air-to-air and air-to-surface gunnery, minesweeping operations, submarine operations, air combat maneuvers, and instrument training (MMS, 1983). These areas, along with the locations of established shipping lanes, are illustrated in Figure 4-1. No estimates for the noise produced by these activities are available.

In addition, there are numerous oil platforms and rigs located on the continental shelf. Most of these are located to the north of the shipping lane that transects the Gulf at approximately 27°30'N.

5.0 Bottom Characteristics

The experiment site is located in what is known as the Northern Gulf of Mexico Province (Antoine, 1972), which includes the continental shelf and slope from the DeSoto Canyon to the United States - Mexico border. The following is a brief description of the experiment area bathymetry, bottom sediments, and geotechnical properties as applied to anchor holding capacity.

5.1 Bathymetry

The experiment site at 26°40'N, 92°30'W lies on the continental slope portion of the Northern Gulf of Mexico Province.

In general, the continental slope in this area is irregular and hammocky, being composed of a random arrangement of depressions and ridges resulting from the action of salt diapirism (Figure 5-1). These features are between 2 and 3 m in depth/height. The experiment site is located near one of these salt-influenced ridges (Figure 5-2), although this particular bathymetric high is less prominent than some of those elsewhere in the general area.

About 40 minutes to the south of the site lies the steep, east-west trending Sigsbee Escarpment, an important bathymetric feature that separates the continental slope from the continental rise and the deep Sigsbee Abyssal Plain. Eroded into the Sigsbee Escarpment are two submarine canyons that flank the southern reaches of the experiment area (Figure 5-1 and 5-2). The western canyon is much more prominent than the eastern, but both can be expected to serve occasionally as sediment transport paths to the abyssal plain. However, the canyons are far enough removed from the area so that the possibility of any sediment movement along these conduits is not a factor in this analysis.

Although the continental slope is marked by a variety of bathymetric features, the slope in the area averages less than 1°.

5.2 Sediments

The sediment information reported here has been taken primarily from Bouma (1972), who carried out a comprehensive study of shallow piston cores taken throughout the Gulf of Mexico during several exercises. The average depth of the cores was 7 m. Enough samples were taken in the experiment area to allow a good understanding of the depositional history of the upper portion of the sedimentary column.

In general, the upper sediments of the outer shelf and slope of the Gulf of Mexico are primarily clay with variable amounts of silt (Bouma, 1972), and are commonly known as pelite. The average percent clay content of the upper sediments in the experiment area is shown in Figure 5-3. The experiment site lies in an area in which the clay content of the surface and near-surface sediments is rather uniform, ranging from 70 to 80 percent of the total sediment volume.

The percent sand content (Figure 5-4) of the sediments in the experiment area is significantly lower than the clay content, which is to be expected in this mid- to deep-water depositional environment. Sand percentage of sediment volume ranges from 0 to 17 percent. Most of the sand-sized particles present are not quartzitic. Instead, they are detrital particles, foraminifera skeletons, and fossil fragments (Bouma, 1972), all of which are mainly carbonate.

The average carbonate content (Figure 5-5) of the upper sedimentary column in the deployment area is relatively low compared to the eastern and southern portions of the Gulf of Mexico (Bouma, 1972), and reflects the lack of a sediment source.

Carbonate material, ranging from 10 to 25 percent of upper sediment volume, is made up primarily of foraminifera tests, assorted detrital particles, and reworked bottom sediment.

Of interest in the study of the upper few meters of sediment in the Gulf is the thickness of Globigerina ooze. Bouma (1972) found that most off-shelf areas in the Gulf of Mexico are covered by at least a thin veneer of ooze, and often much more. Many times, this covering will mask other sediment types which might have significantly different geotechnical properties. However, the experiment site appears to be free of Globigerina ooze (Figure 5-6), except for a rather thick but isolated deposit to the west. This localized accumulation is probably influenced by the prominent bathymetric low which cuts into the Sigsbee Escarpment at approximately 26°15'N, 93°20'W (Figure 5-2). This low serves as a basin to trap the ooze and allow a thicker deposit to form than what is observed in the immediately surrounding area.

5.3 Sediment Shear Strength

Rocker (1985) developed an equation for anchor holding capacity in which the critical parameters are first, the characteristics of the anchor being used, and second, the shear strength of the sediment in which the anchor is dropped. Shear strength has been measured in a core taken very close to the experiment site (Bryant and Wallin, 1968) (Figure 5-7). The measurement was determined by a motorized vane-shear apparatus that has a constant rotation of 12 degrees per minute. A two-bladed vane, 0.5 in long and 0.5 in wide, and buried to a depth of 1 in below the surface of the core was used to shear the sediment. The results of the measurement are given in Figure 5-8. This plot of undrained shear strength versus depth shows a rather consistent shear strength for the first 2 meters of 4.3 kPa and then a rapid increase with depth. Based on findings by Bryant and Wallin (1968), the increase in shear strength with depth is probably due to a very slow rate of deposition, which allows a longer period of consolidation. They suggest that this is typical for a far-shelf to continental slope environment far removed from rich sediment sources.

It appears, then, that 4.3 kPa is a reliable estimate of undrained shear strength for calculating anchor holding capacity at the experiment site.

5.4 Summary

The experiment site is located in the Northern Gulf of Mexico Province (Antoine, 1972) and lies on the far continental slope just north of the Sigsbee Escarpment. The bathymetry is strongly influenced by salt diapirism, resulting in an irregular arrangement of depressions and ridges. On a subregional scale, however, the bathymetry is rather gentle, with a slope that averages less than 1°.

The upper portion of the sedimentary column is mostly clay (70 to 80 percent of total sediment volume), with lesser amounts of

sand and carbonate material. Most of the sand-sized particles consist of broken foraminiferal tests, detrital particles, and microfossil skeletons. Whereas a thin veneer of Globigerina ooze covers much of the deeper portions of the Gulf of Mexico, the experiment site is free from any deposit of ooze.

Measurement of undrained shear strength in a core very close to the experiment site gives a value of 4.3 kPa which can be used in the calculation of anchor holding capacity.

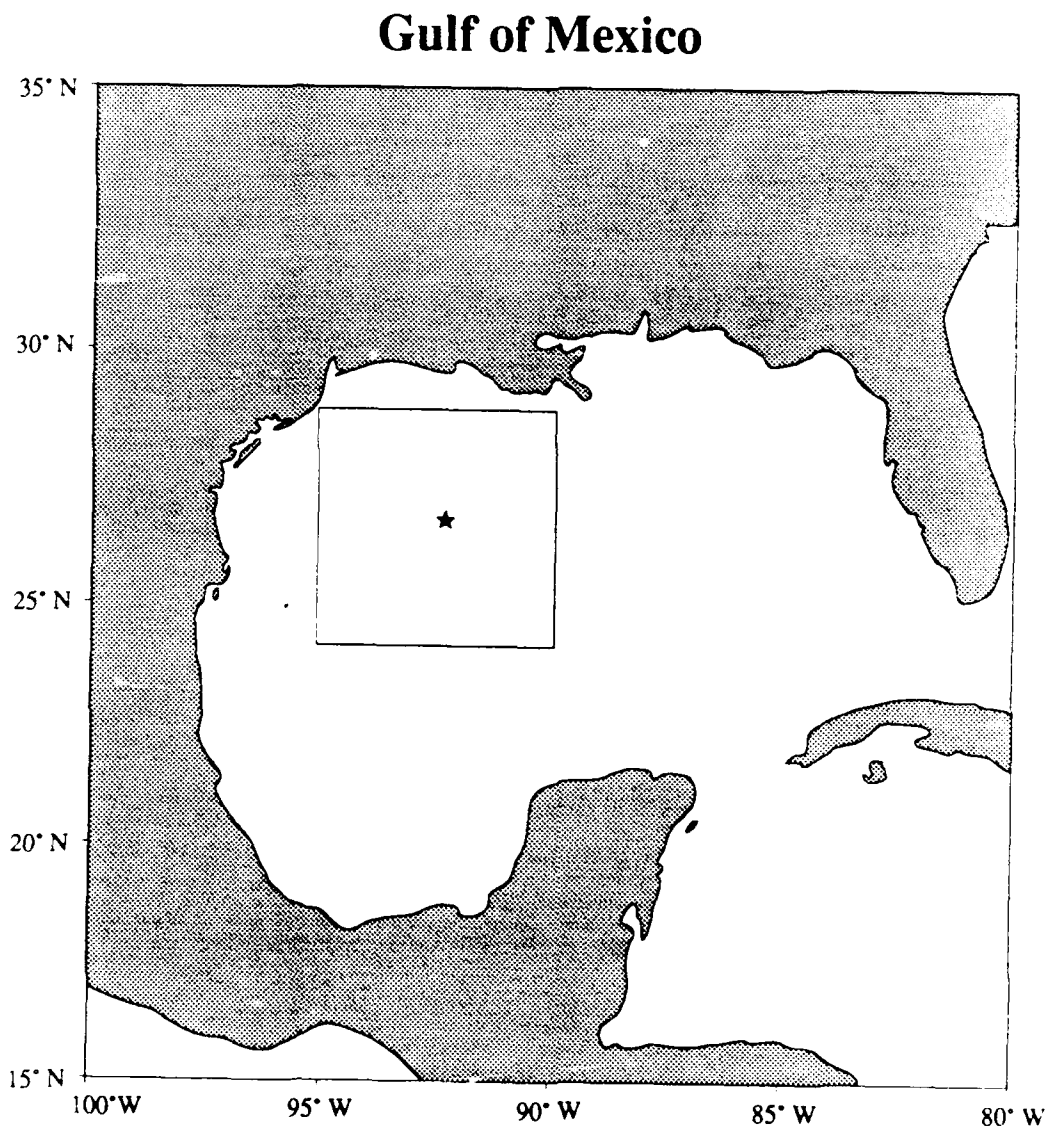

Figure 1-1. Area of interest and location of experiment site.

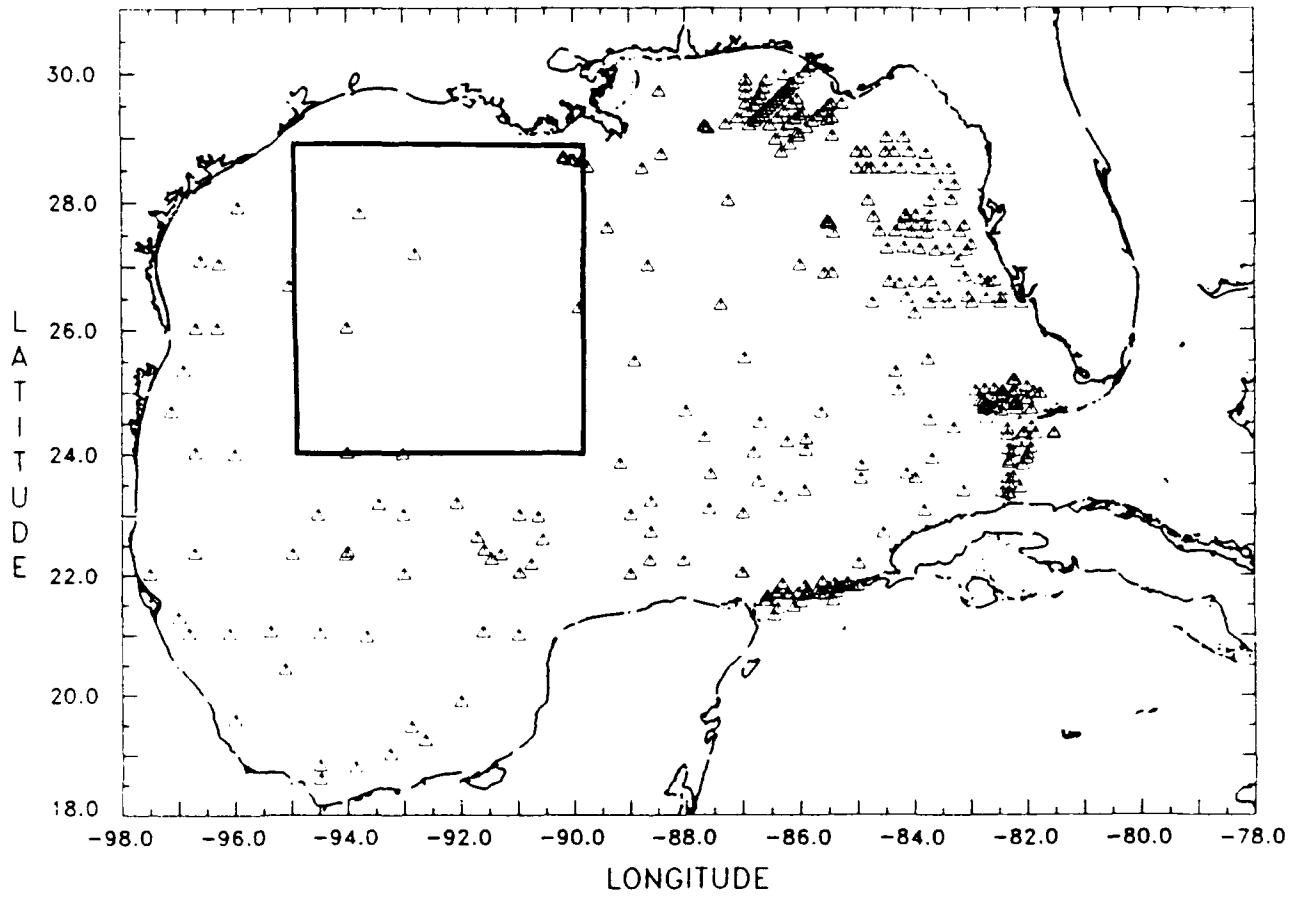

Figure 2-1. Station locations of temperature and salinity data extracted from MOODS. Box indicates area of interest.

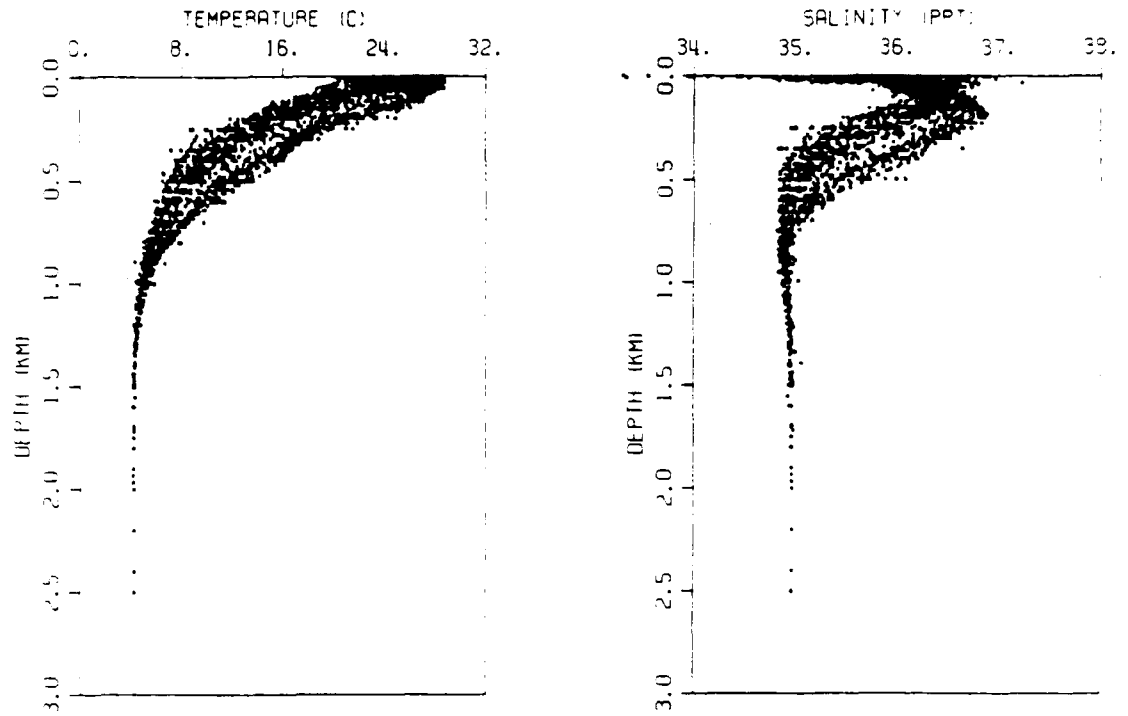

Figure 2-2. Temperature and salinity profiles for the month of November from MOODS. Data were extracted from the area of interest indicated by the box in Figure 2-1.

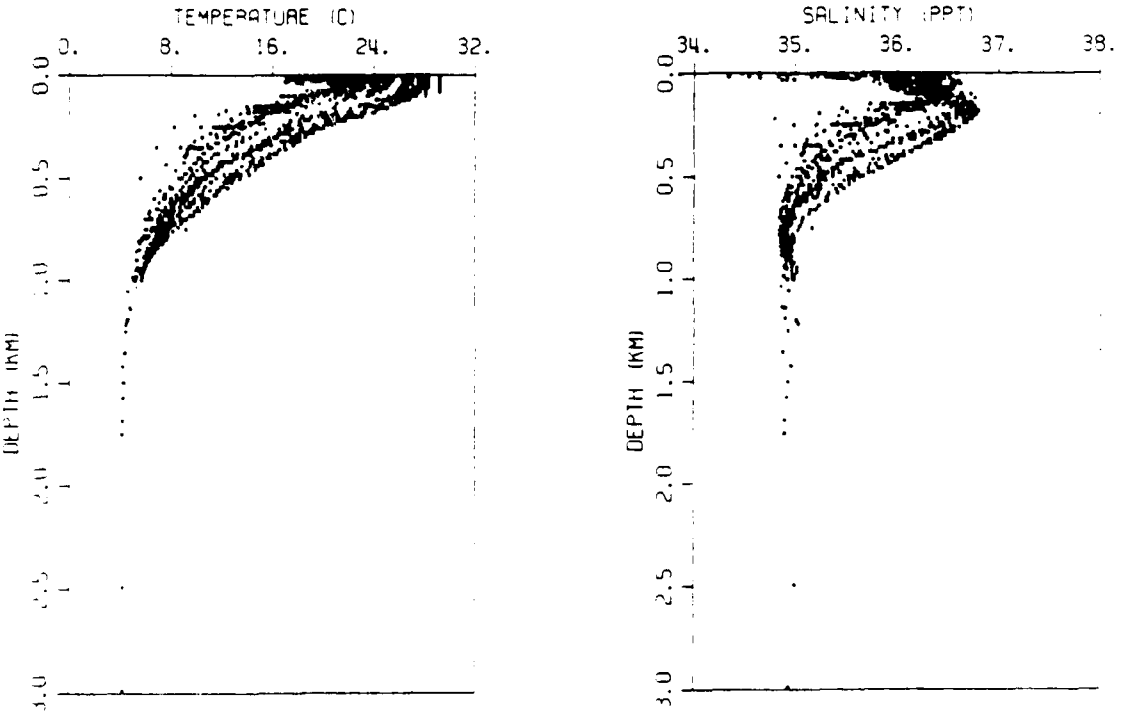

Figure 2-3. Temperature and salinity profiles for the month of December from MOODS. Data were extracted from the area of interest indicated by the box in Figure 2-1.

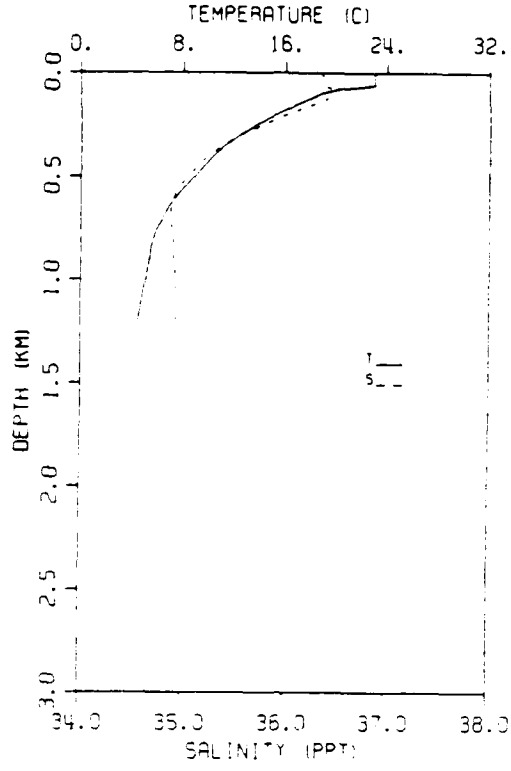

Figure 2-4. Most commonly occurring temperature (solid) and salinity (dashed) profiles from MOODS (December).

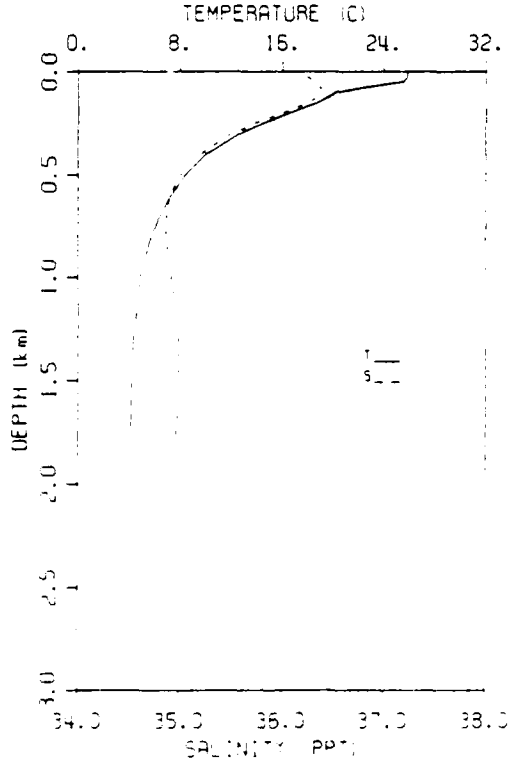

Figure 2-5. Temperature (solid) and salinity (dashed) profiles from GDEM for the experiment site.

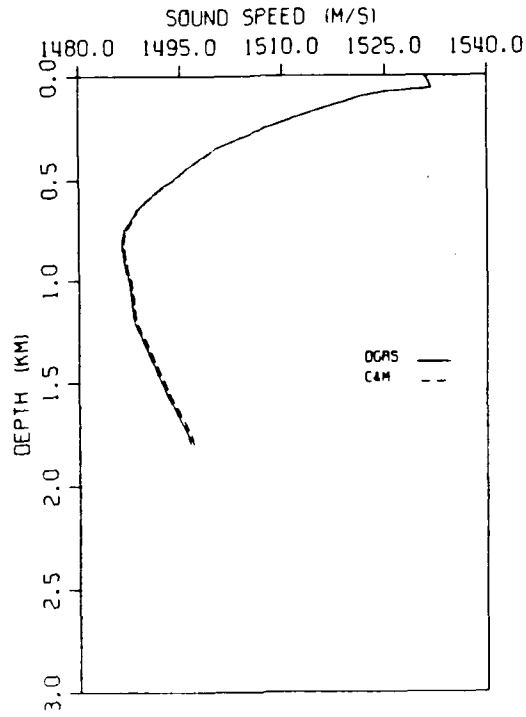

Figure 2-6. Sound speed profiles as determined from the most commonly occurring temperature and salinity values shown in Figure 5-4. (Solid - DelGrosso equation, dashed - Chen and Millero equation).

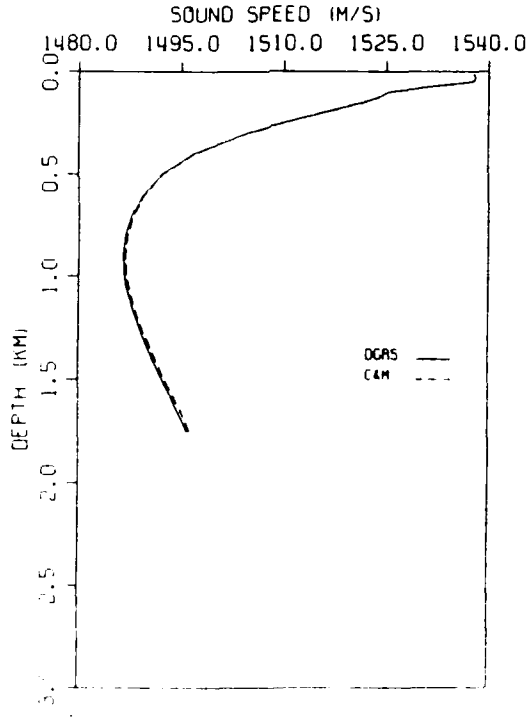

Figure 2-7. Sound speed profile determined from GDEM data at the example site. (Solid - DelGrosso equation, dashed - Chen and Millero equation).

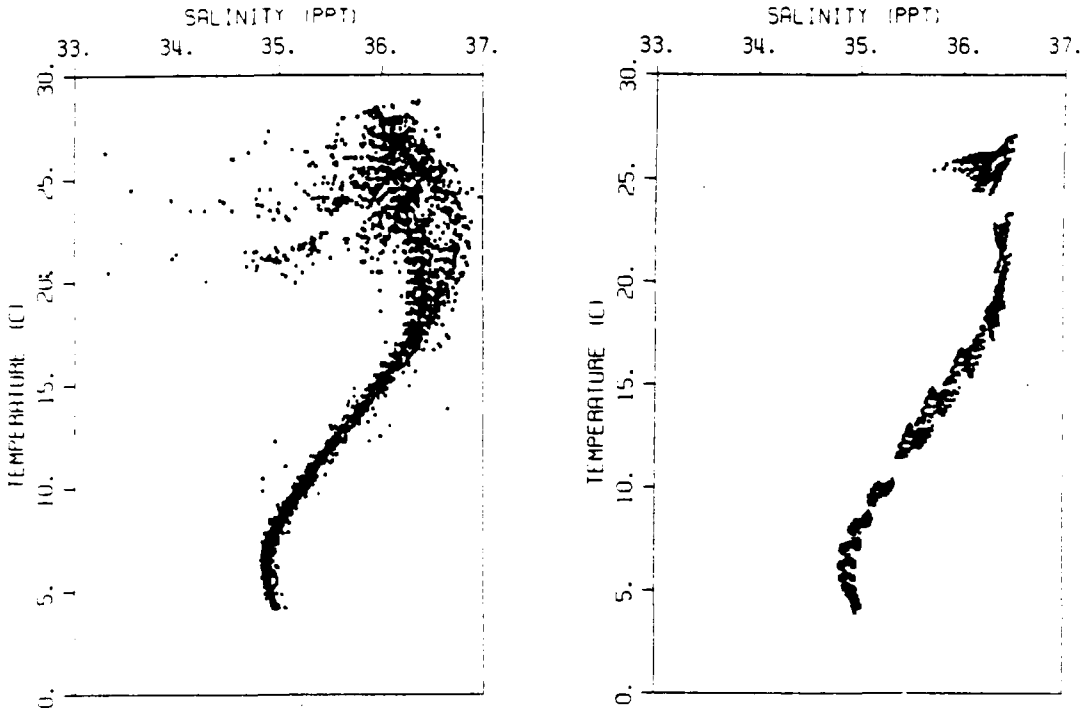

Figure 2-8. (Left) T-S diagram for MOODS data for the month of November. (Right) T-S diagram for GDEM for the autumn. Both diagrams contain data extracted from the box indicated in Figure 2-1.

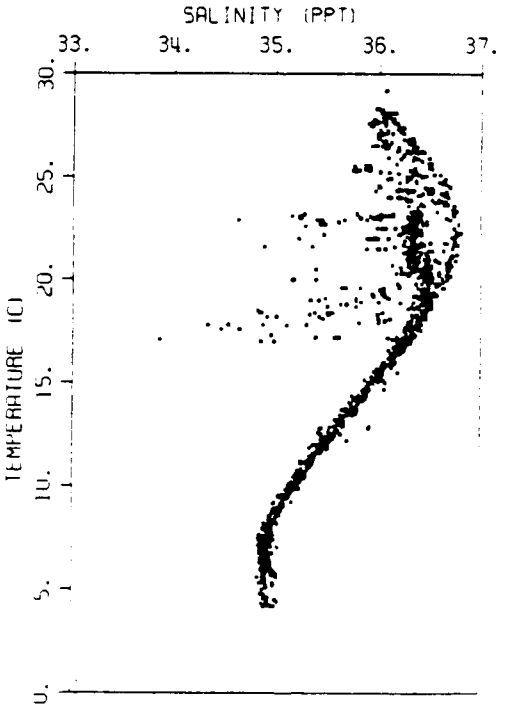

Figure 2-9. T-S diagram for MOODS data from the box indicated in Figure 2-1 for the month of December.

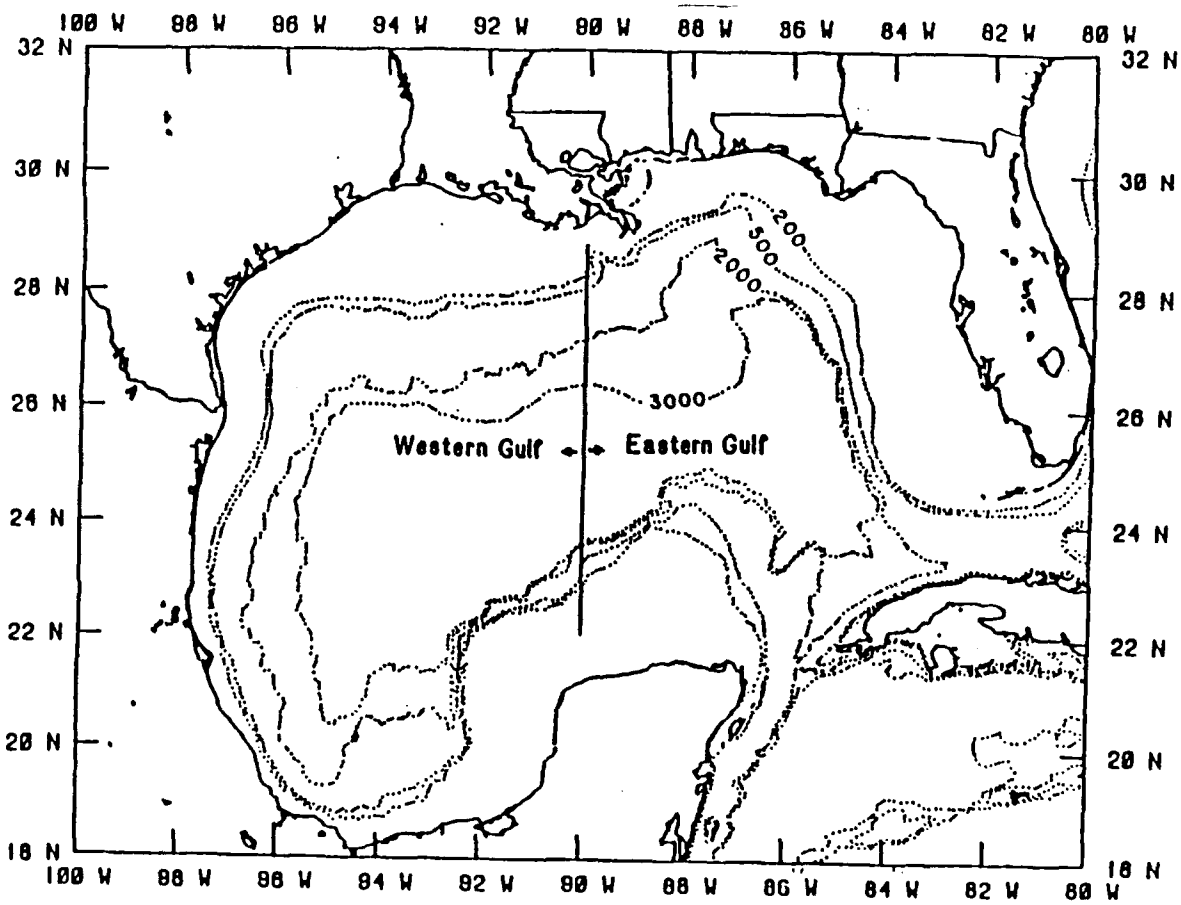

Figure 2-10. Partitions of the Gulf of Mexico as referenced throughout the text of this technical note (after MMS, 1986).

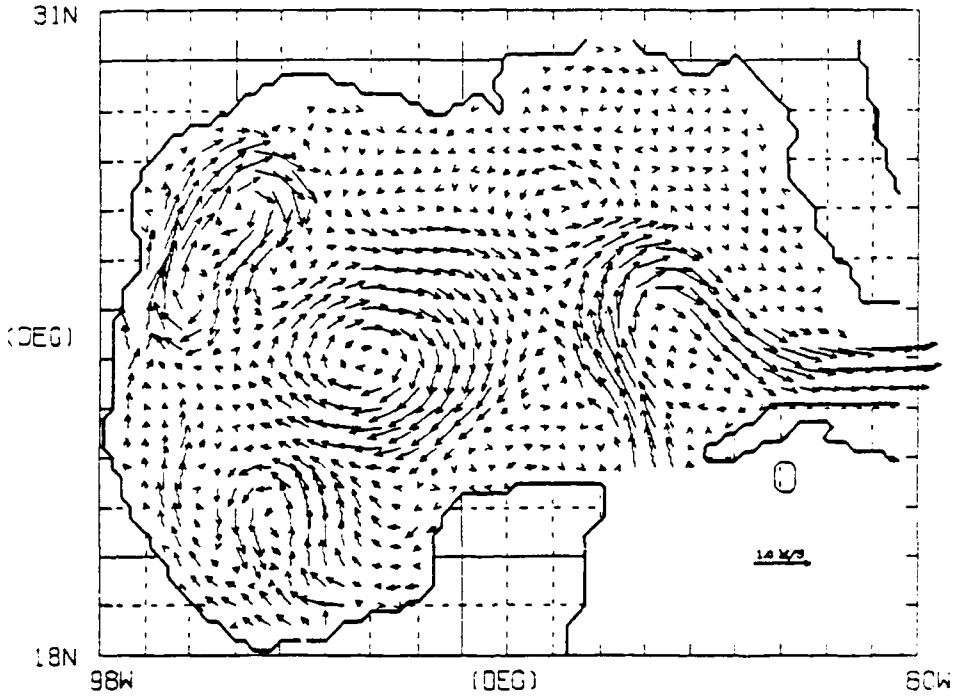

Figure 2-11. Numerical simulation of the general circulation in the Gulf of Mexico (after Wallcroft, 1984). Results of model developed from available data sets. Winter representation.

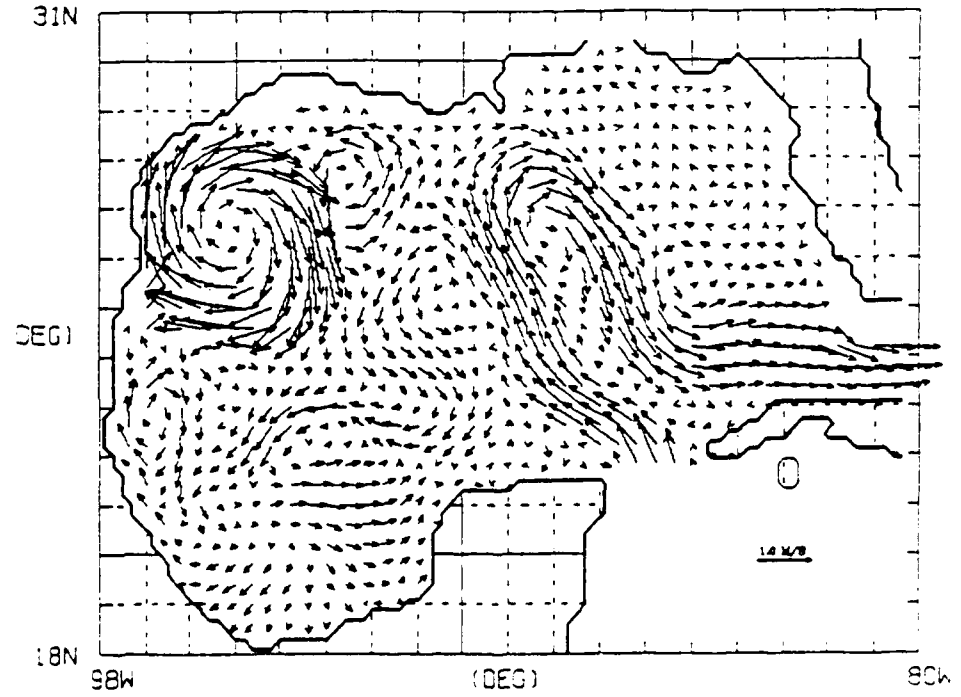

Figure 2-12. Numerical simulation of the general circulation in the Gulf of Mexico (after Wallcroft, 1984). Results of model developed from available data sets. Summer representation.

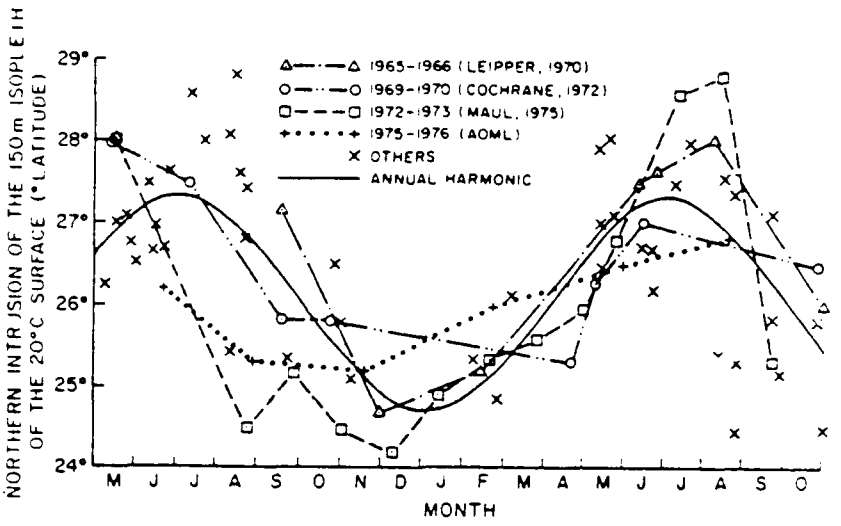

Figure 2-13. Penetration of the Loop Current into the Gulf as determined by month for each of four data sets (after Behringer et al., 1977).

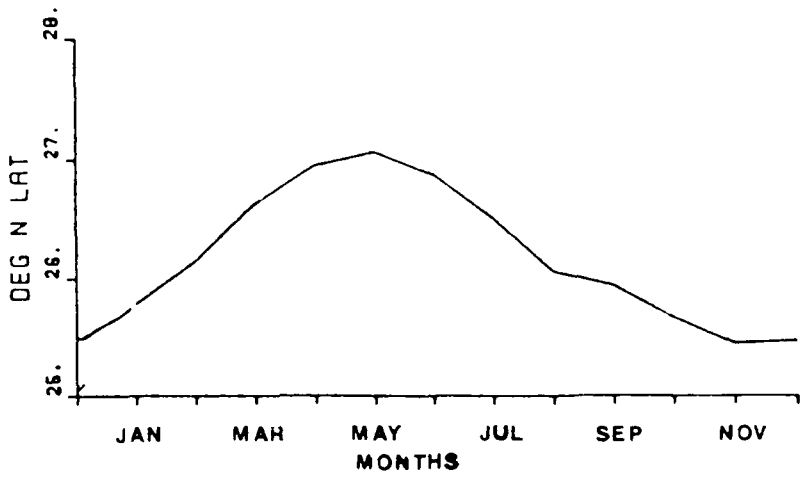

Figure 2-14. Average annual northern extent of the Loop Current (after Sturges and Evans, 1983).

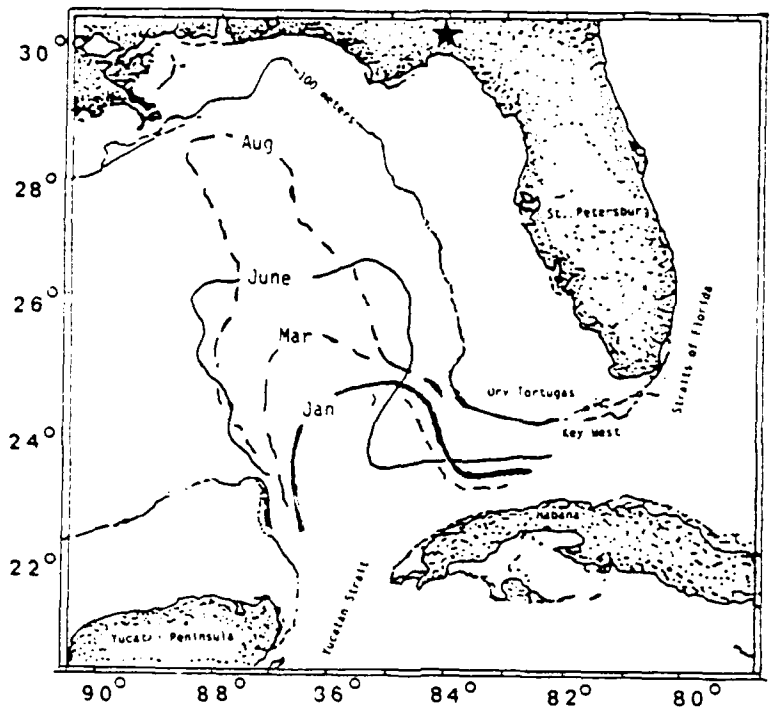

Figure 2-15. Average annual development of the Loop Current (after Sturges and Evans, 1983).

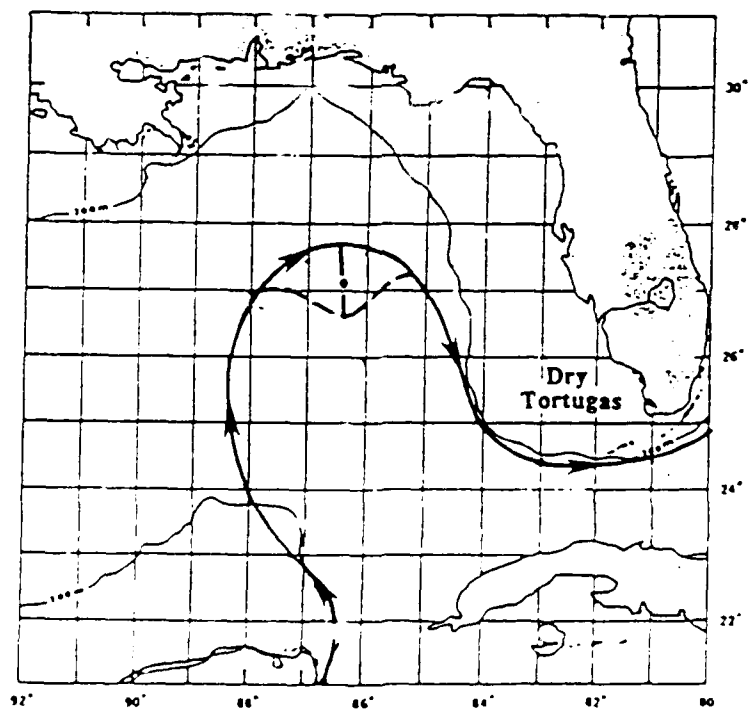

Figure 2-16. Average position of the Loop Current boundary (after Vukovich, 1988).

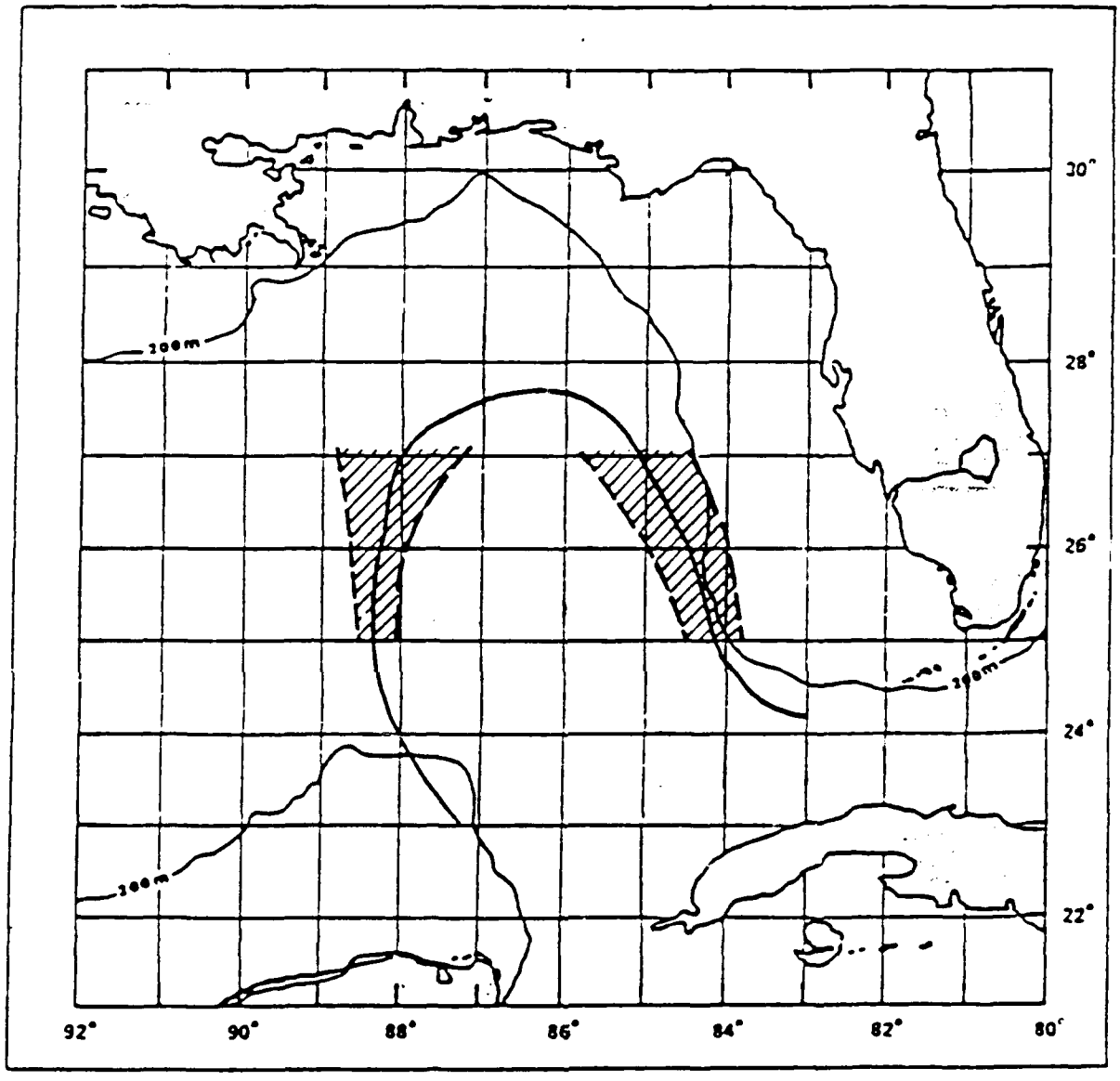

Figure 2-17. Variation of the eastern and western boundaries of the Loop Current between 25° and 27°N (after MMS, 1986).

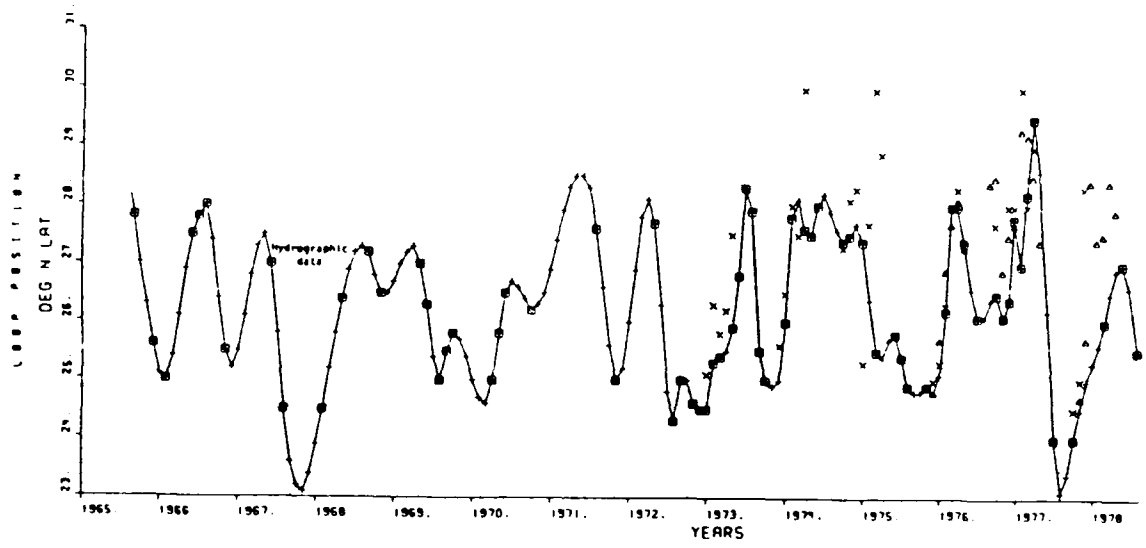

Figure 2-18. Position of the northern boundary of the Loop Current (after Sturges and Evans, 1983).

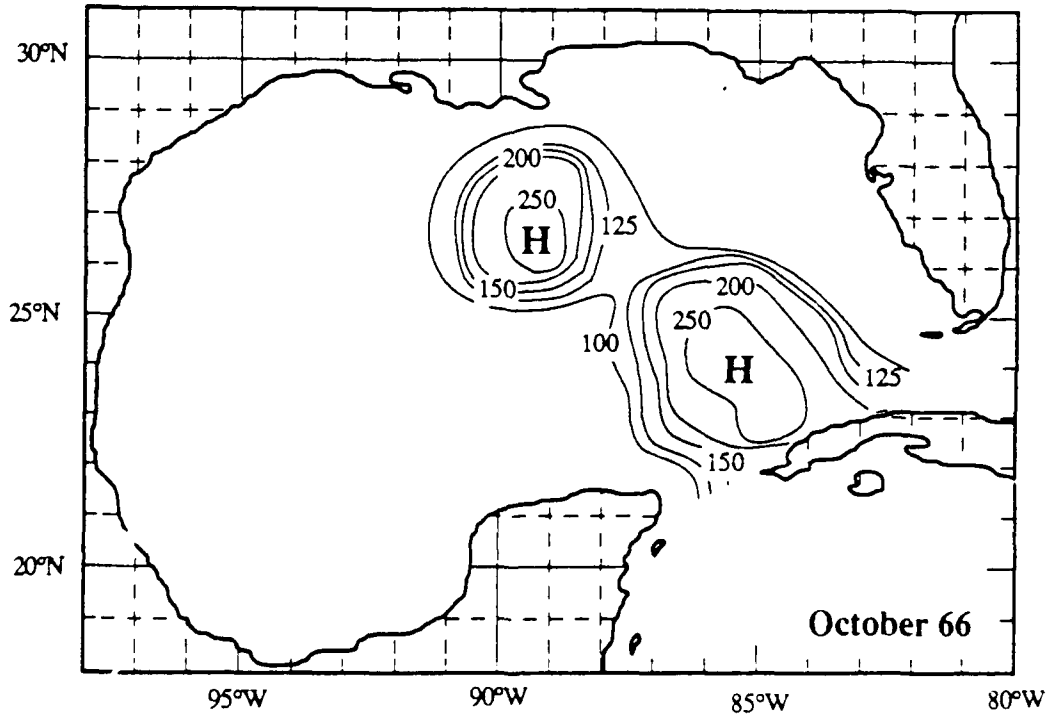

Figure 2-19a. Eddy formation at most northerly extent of Loop Current (after Wallcroft, 1984). Contours represent the depth (m) of the 22°C isotherm.

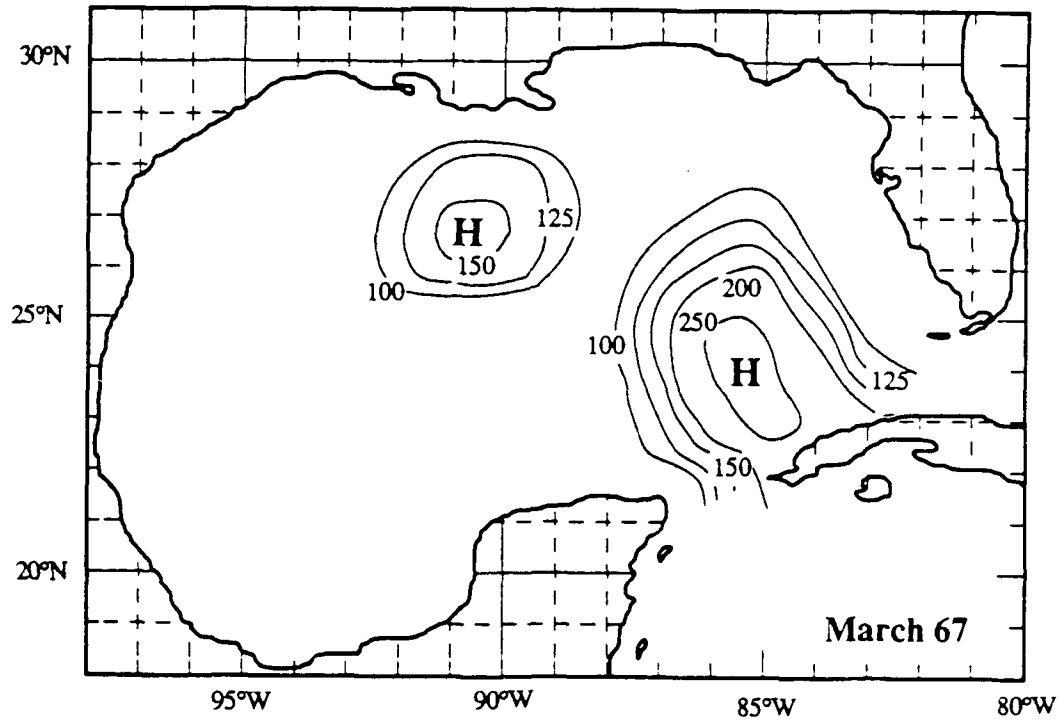

Figure 2-19b. Detached eddy moving across Gulf (after Wallcroft, 1984). Contours represent the depth (m) of the 22°C isotherm.

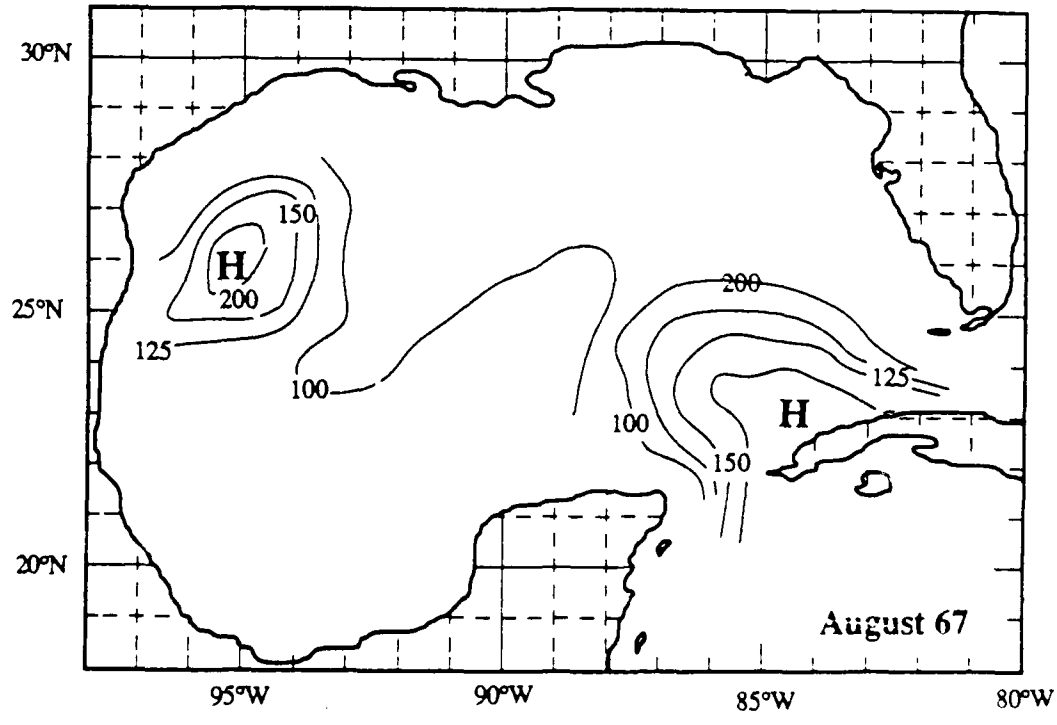

Figure 2-19c. Eddy reaching Mexican coast (after Wallcroft, 1984). Contours represent the depth (m) of the 22°C isotherm.

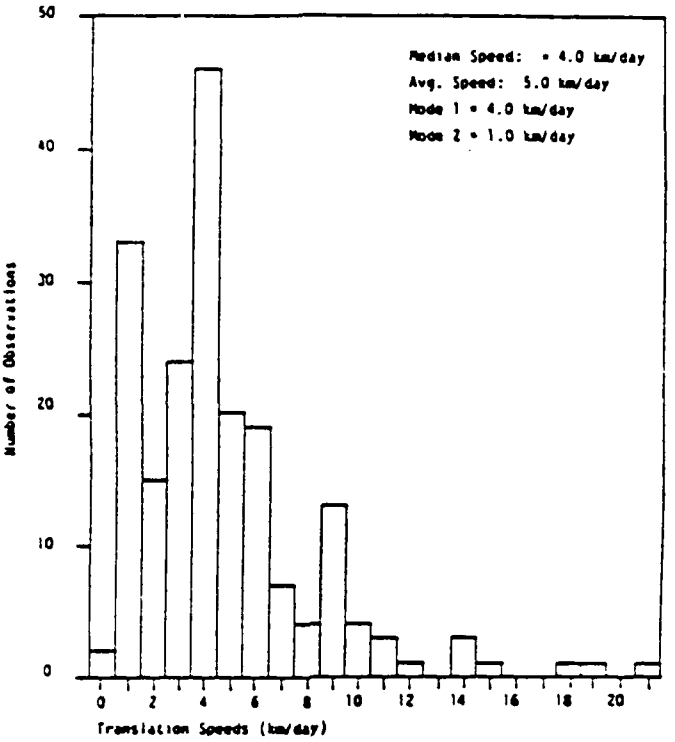

Figure 2-20. Frequency distribution of eddy translation speeds (after MMS, 1986).

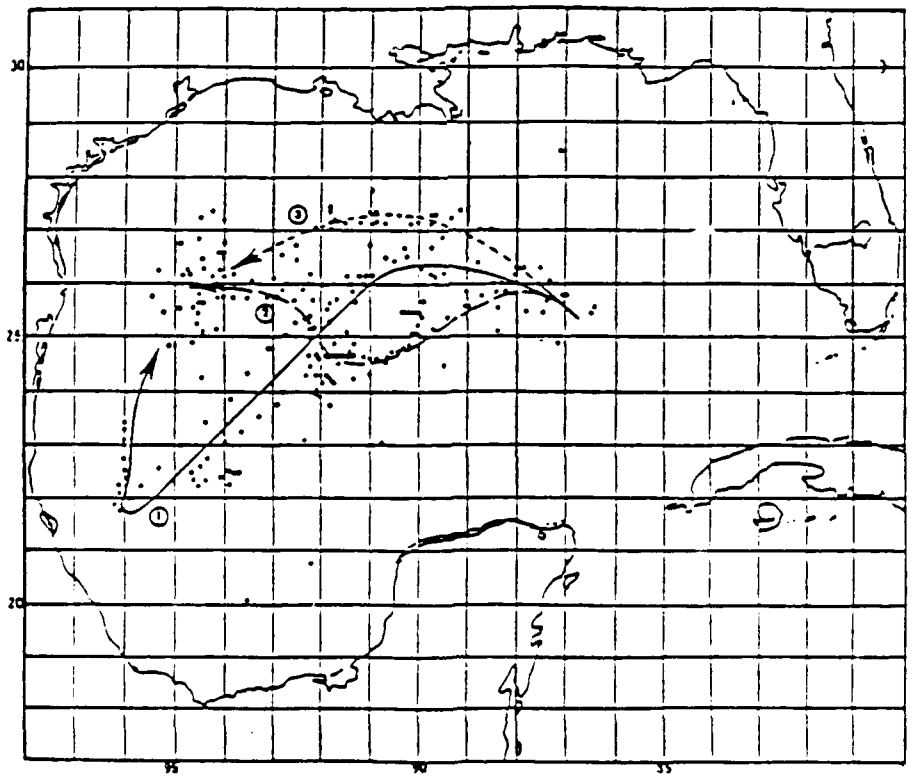

Figure 2-21. Typical paths of Loop Current eddies (after MMS, 1986).

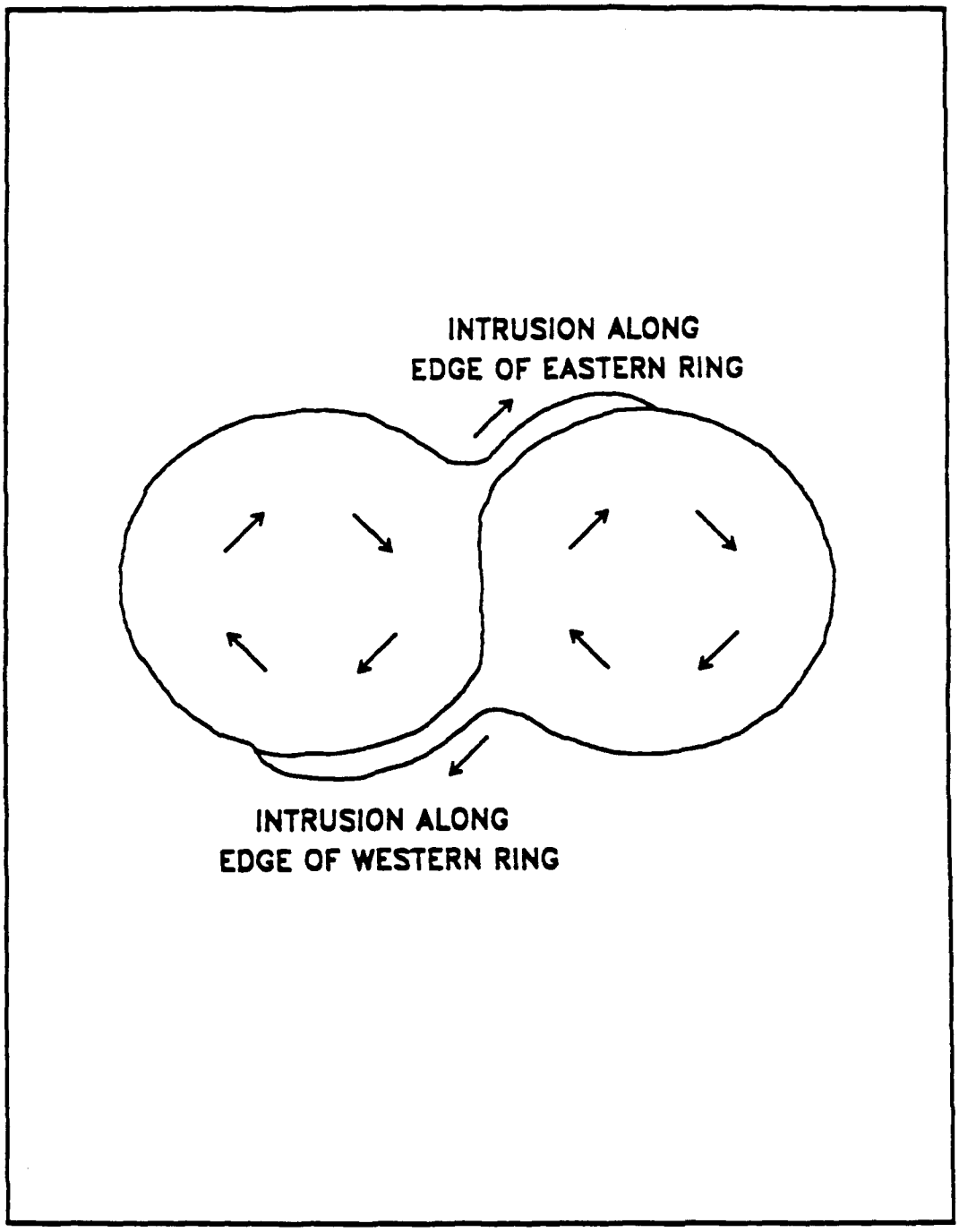

Figure 2-22. Depiction of coalescing eddies (from SAIC, 1989).

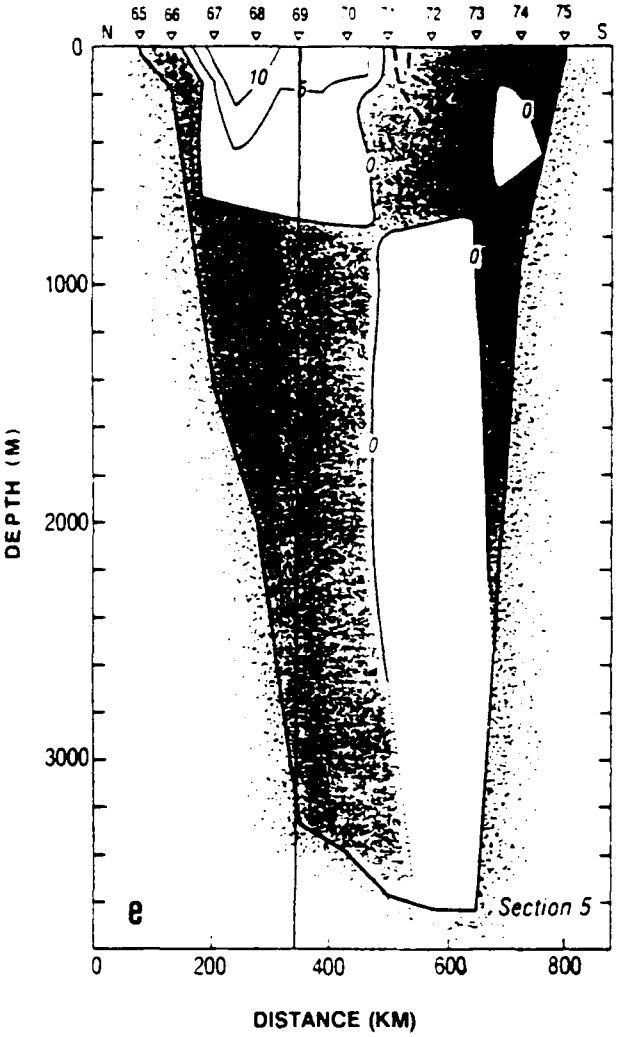

Figure 2-23. Average geostrophic currents at the experiment site (after Hofmann and Worley, 1986). Values are in cm s^{-1}. Clear areas indicate currents flowing toward the east. Shaded areas indicate currents flowing toward the west.

GULF OF MEXICO WAVE DIRECTION

WAVE HEIGHT(M)

WAVE DIRECTION	0	1	2	3	4	6	8	10	12	14+	TOTAL %
N	2	8	3	1	+						14
NE	4	11	3	1	+						19
E	5	16	4	+	+						25
SE	3	11	3	+	+						17
S	2	4	1	+	+						7
SW	1	1	+	+	+						2
W	1	1	+	+	+						2
NW	2	5	2	1	+	+					10
CALM	3	+		+							3
TOTAL %	22	57	17	3							

+ = <.5%

Total Number of Observations: 6787

Figure 2-24. Frequency of surface waves by height and direction. Numbers in bins are %. The direction given indicates the direction from which waves are coming. Data are from all averaged sea wave observations available prior to 1975.

GULF OF MEXICO WINDS

WIND SPEED (KNOTS)

WIND DIRECTION	0	4	7	11	17	22	28	34	41	48+	TOTAL %
N	+	1	3	4	3	1	+	+	+		14
NE	+	1	5	7	4	1	+	+		+	19
E	+	2	6	10	5	1	+	+			24
SE	+	1	4	7	4	1	+	+			18
S	+	1	2	3	1	1	+	+			9
SW	+	+	1	1	+	+	+	+			2
W	+	1	1	1	1	+	+	+		+	4
NW	+	1	2	3	2	1	+	+	+		9
CALM	1										1
TOTAL %	4	9	23	35	[illegible]	7	2	+	+		

+ = <.5%

Total Number of Observations: 8176

Figure 3-1. Frequency of occurrence of wind speed and direction. Numbers in bins are %. Directions given indicate the direction from which the wind is coming.

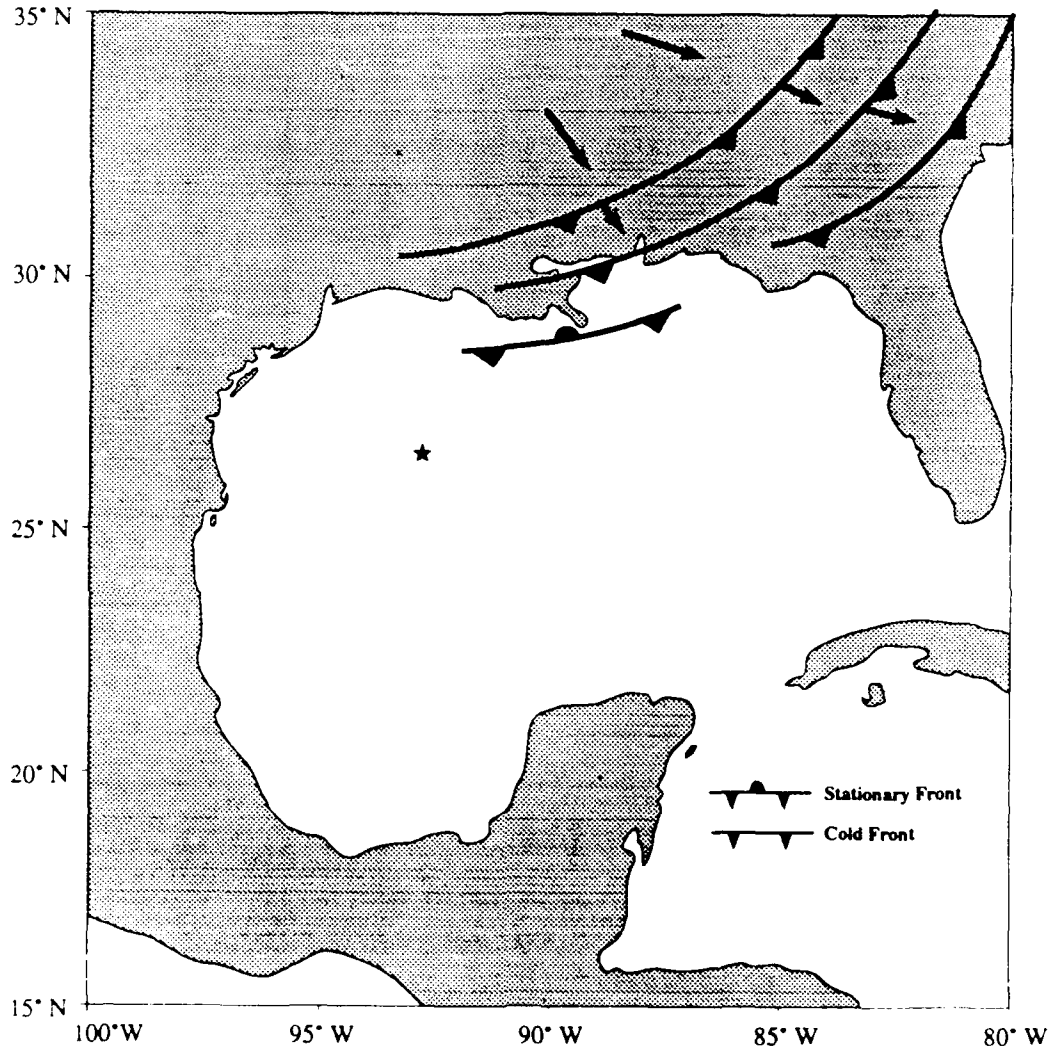

Figure 3-2. Typical cold front track and area of stationary front formation. Experiment site is indicated by a star.

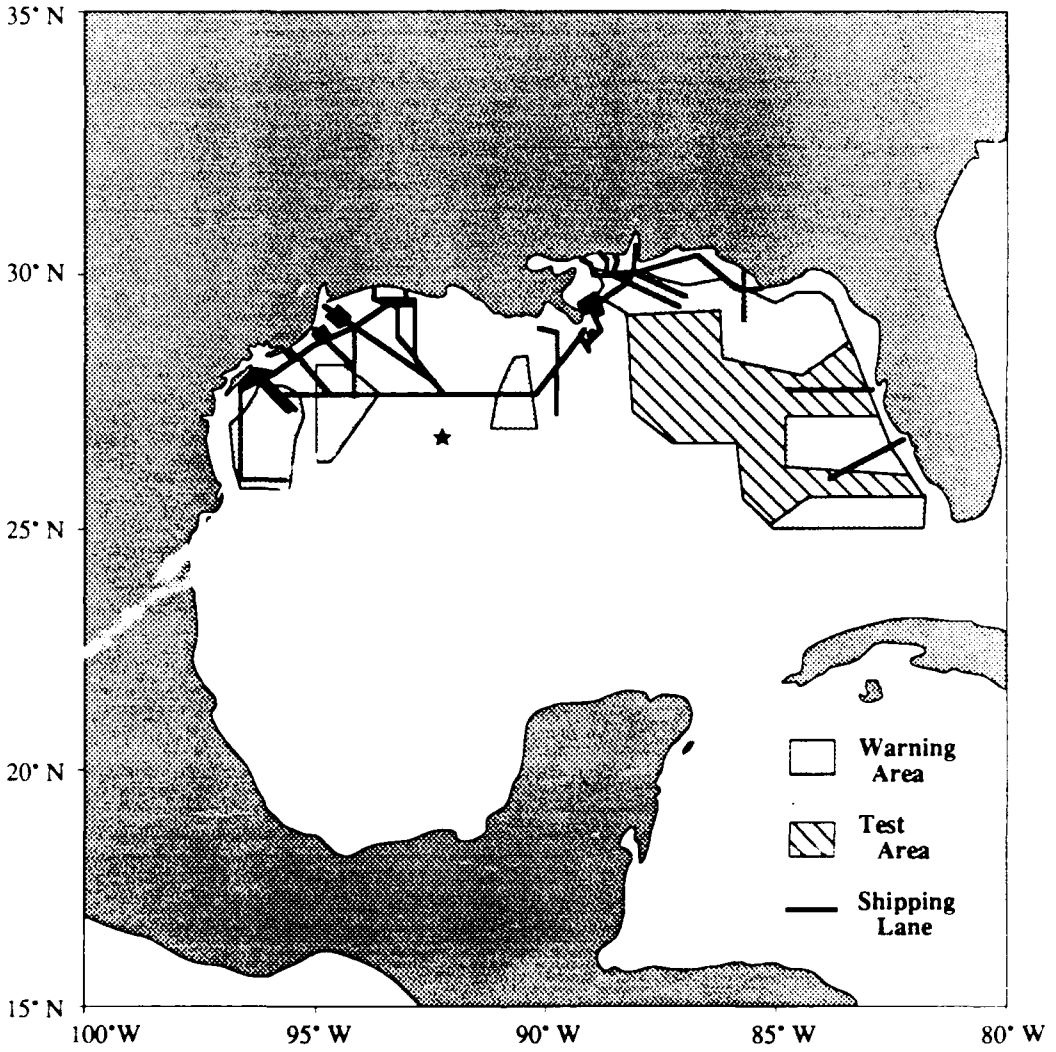

Figure 4-1. Warning areas and shipping lanes in the Gulf of Mexico (from MMS, 1983). Experiment site is indicated by a star.

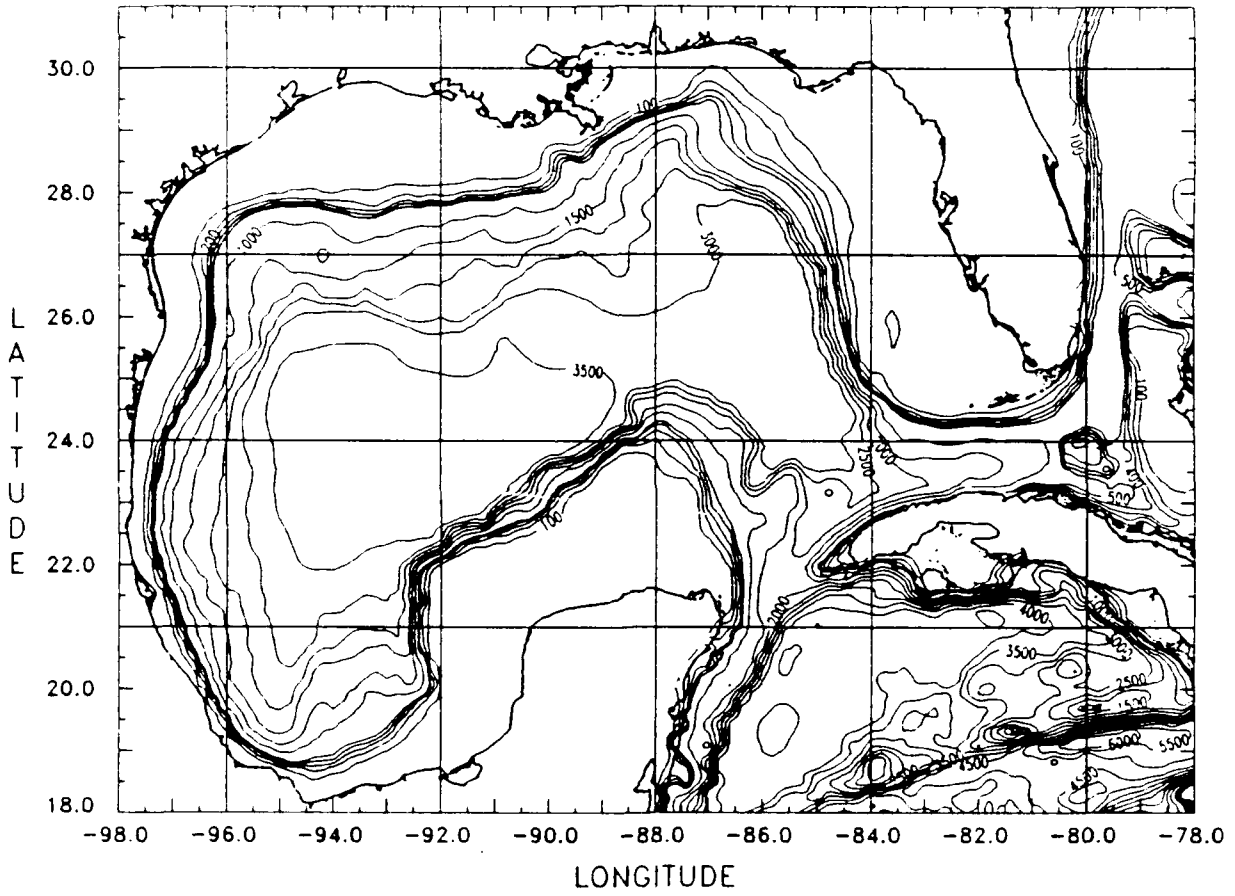

Figure 5-1. Bathymetry of the Gulf of Mexico.

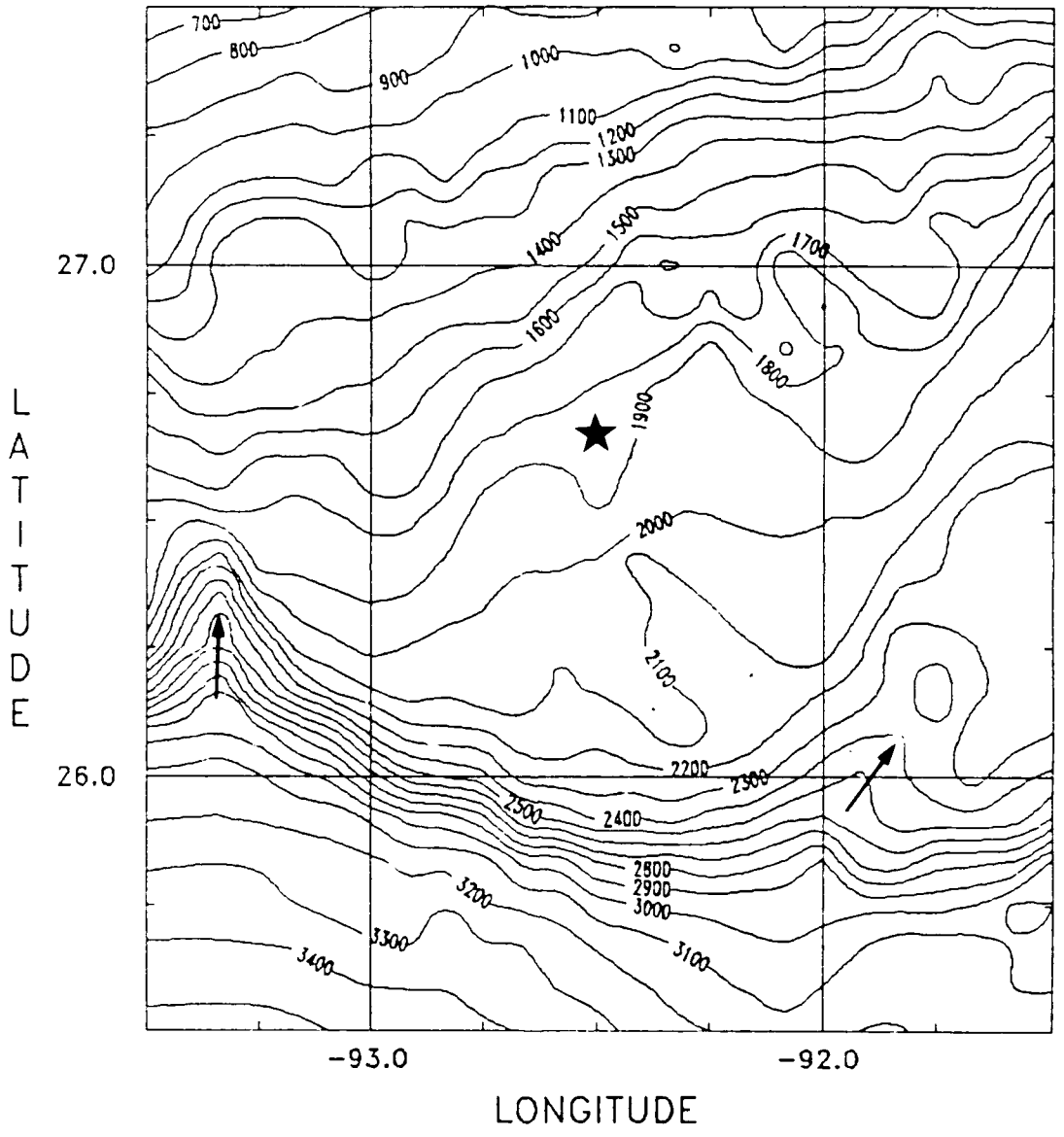

Figure 5-2. Bathymetry near the experiment site. The site is indicated by a star. Submarine canyons are indicated by arrows.

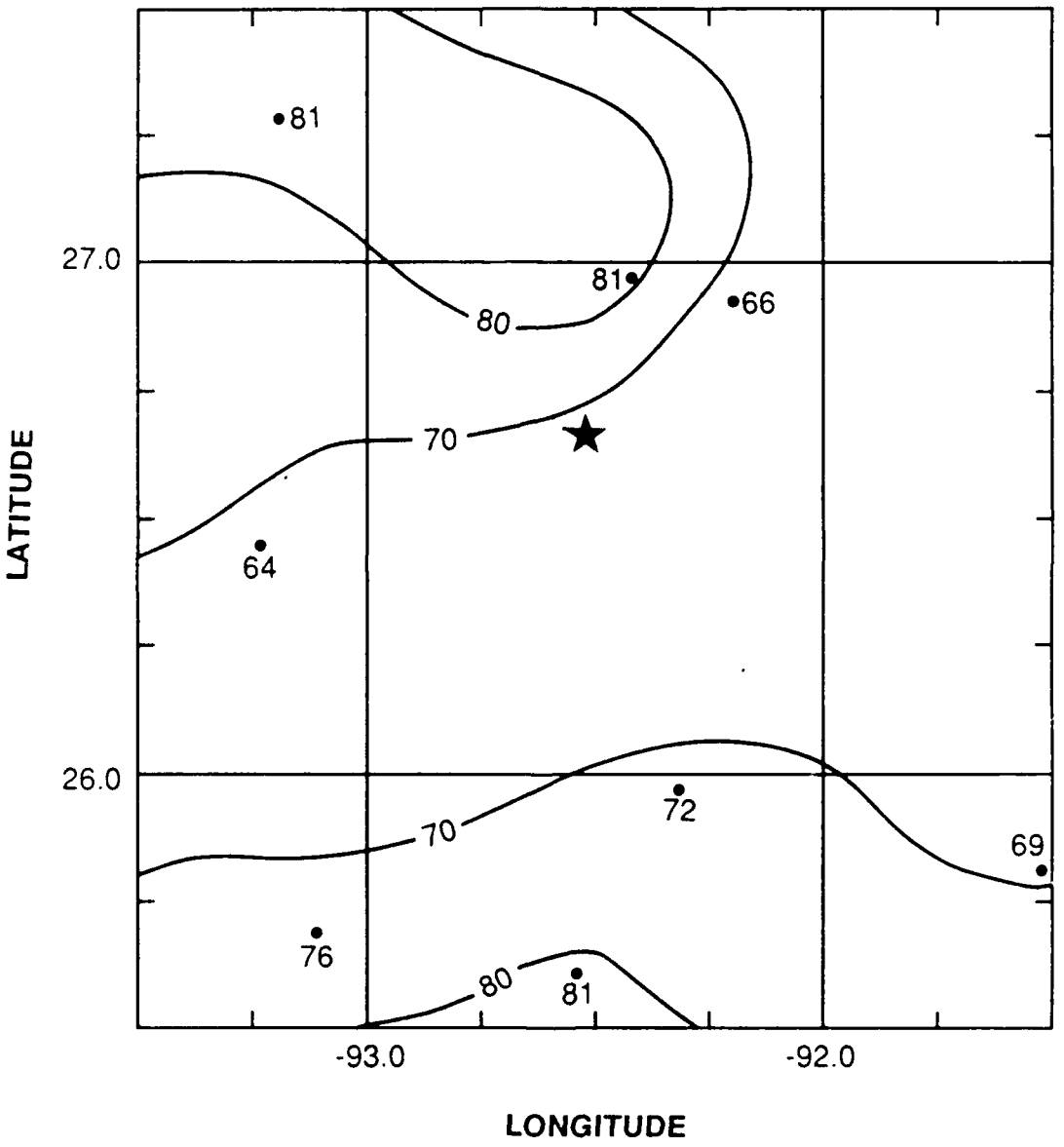

Figure 5-3. Percent clay content of sediments near the experiment site (determined from Bouma, 1972). Contours are in %. The experiment site is indicated by a star.

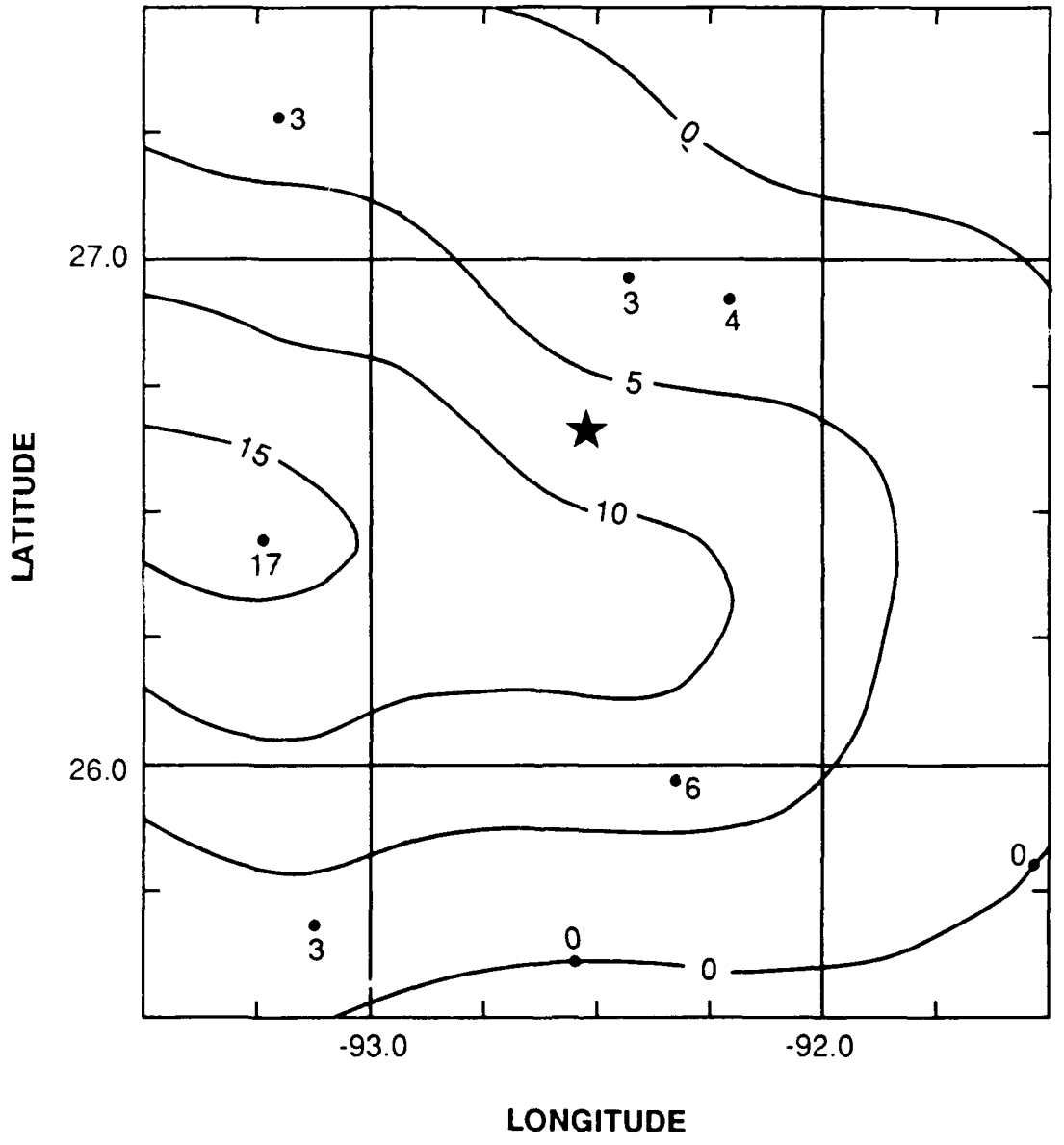

Figure 5-4. Percent sand content of sediments near the experiment site (determined from Bouma, 1972). Contours are in %. The experiment site is indicated by a star.

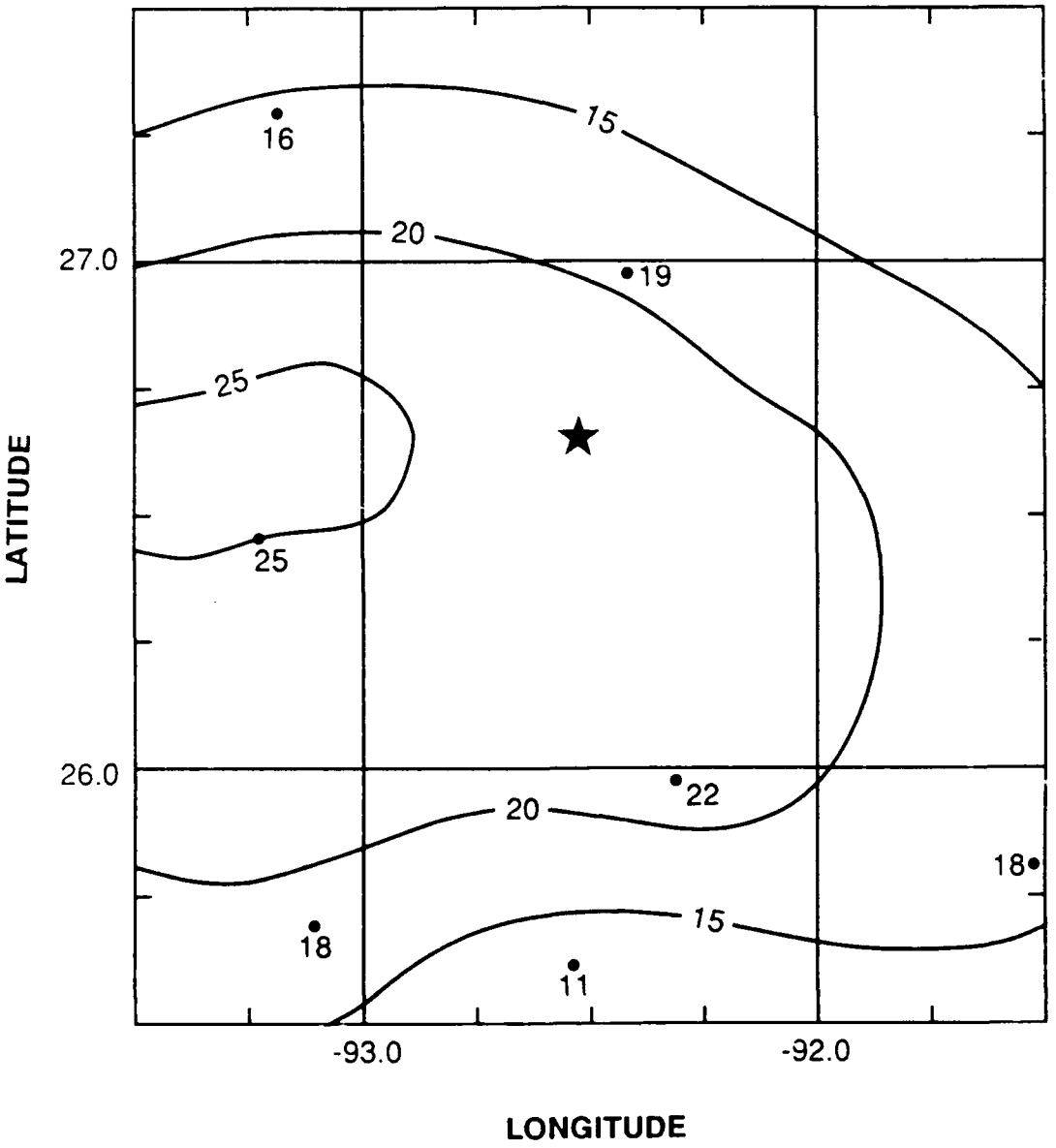

Figure 5-5. Percent carbonate content of sediments near the experiment site. Contours are in %. The experiment site is indicated by a star.

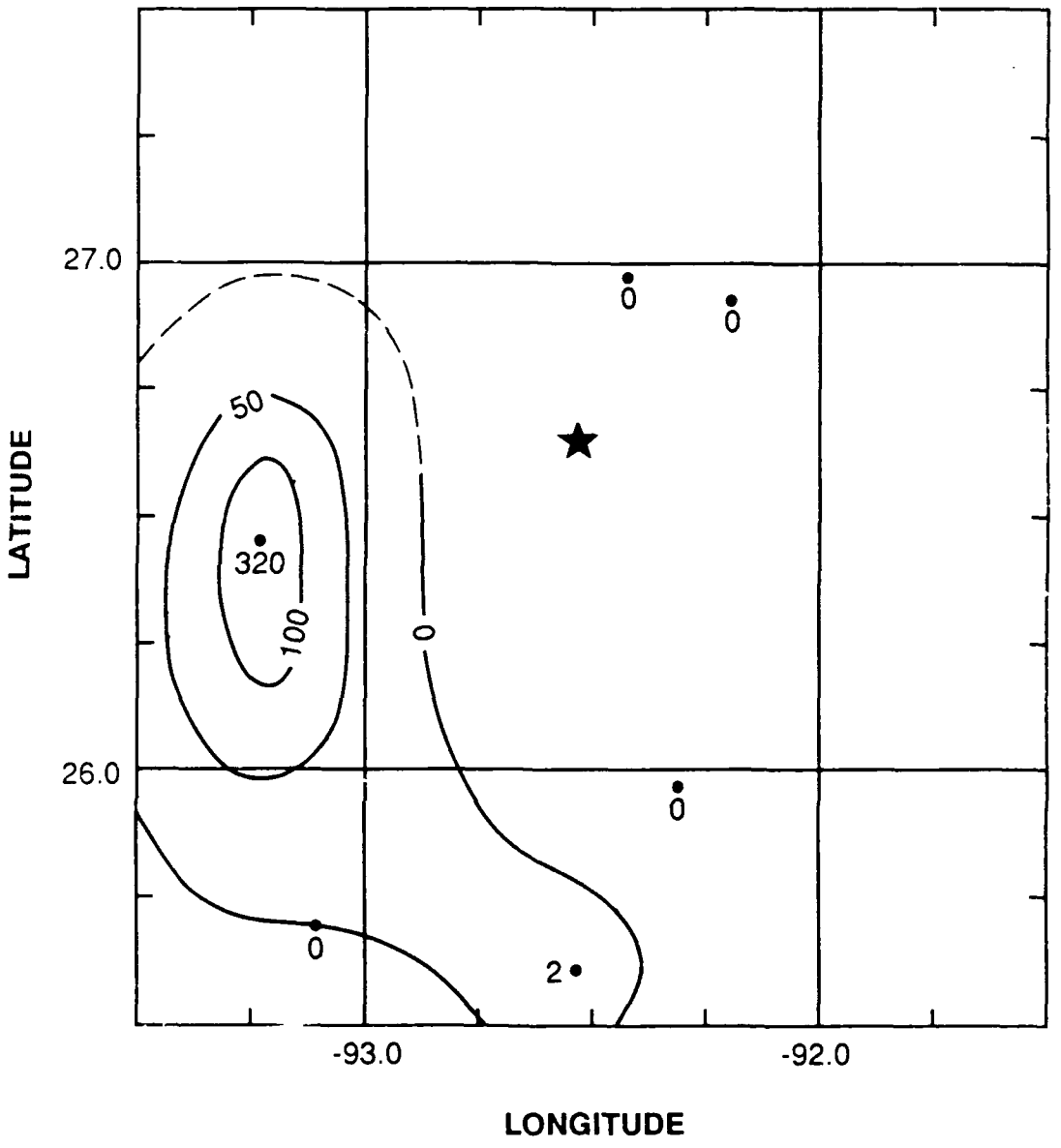

Figure 5-6. Isopach map of Globigerina ooze content of sediments near the experiment site. Contours are in cm and indicate thickness of Globigerina ooze. Experiment site is indicated by a star.

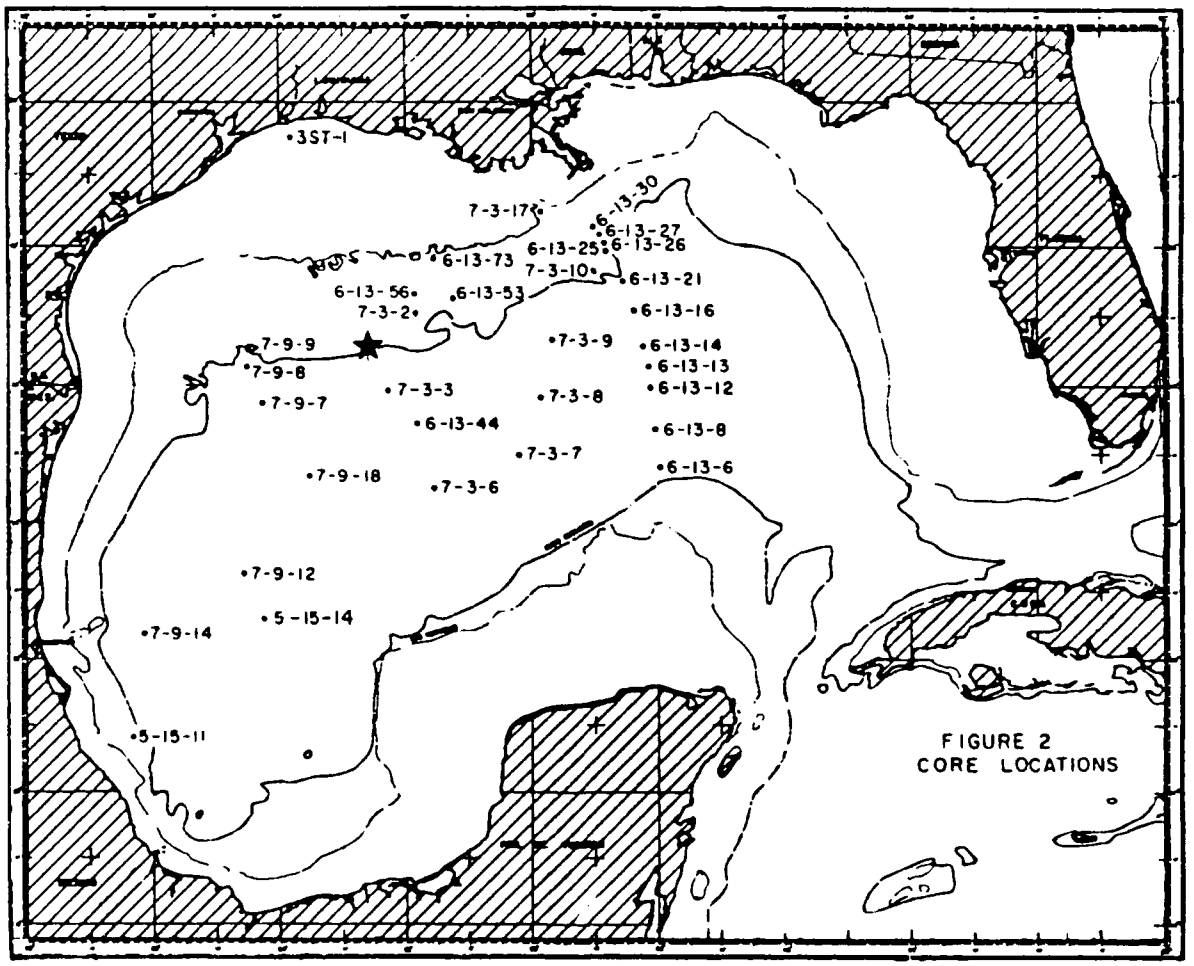

Figure 5-7. Station location map of core samples (from Bryant and Wallin, 1968). Experiment site is indicated by a star.

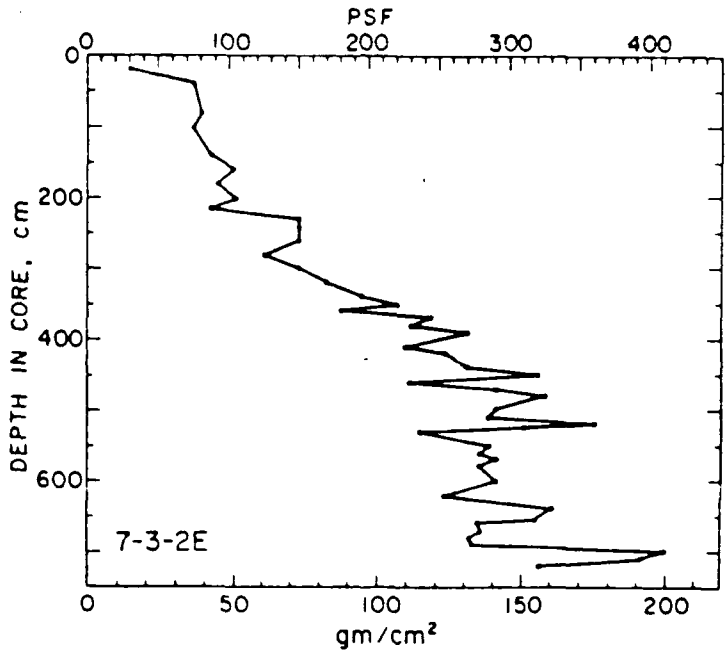

Figure 5-8. Shear strength versus depth for the core sample closest to the experiment site (from Bryant and Wallin, 1968).

6.0 References

Antoine, J.W. (1972). Structure of the Gulf of Mexico. In: Contributions on the Geological and Geophysical Oceanography of the Gulf of Mexico, R. Rezak and V.J. Henry, Eds. Gulf Publishing Company, Houston, TX.

Behringer, D.W., R.L. Molinari, and J.F. Festa (1977). The Variability of Anticyclonic Patterns in the Gulf of Mexico, Journal of Geophysical Research 82(34): 5469-5476.

Bouma, A.H. (1972). Distribution of Sediments and Sedimentary Structure in the Gulf of Mexico. In: Contributions on the Geological and Geophysical Oceanography of the Gulf of Mexico, R. Rezak and V.J. Henry, Eds. Gulf Publishing Co., Houston, TX.

Bryant, W.R., and Wallin, C.S. (1968). Stability and Geotechnical Characteristics of Marine Sediments, Gulf of Mexico. Transactions - Gulf Coast Association of Geological Societies, Vol. XVIII, pp. 334-356.

Defense Mapping Agency (1976). Sailing Directions (Planning Guide) for the North Atlantic Ocean, Defense Mapping Agency Hydrographic/Topographic Center, DMA Stock No. SDPUB140, 164 pp.

DelGrosso, V.A. (1973). Tables of the Speed of Sound in Open Ocean Water, Journal of the Acoustical Society of America 53(5): 1384-1401.

Elliot, B.A. (1982). Anticyclonic Rings in the Gulf of Mexico, Journal of Physical Oceanography 12: 1292-1309.

Fofonoff, N.P. and R.C. Millard (1983). Algorithms for the Computation of Fundamental Properties of Seawater, UNESCO Technical Papers in Marine Science, Number 44, 53 pp.

Forrestall, G. (1990). Eddy Currents, September 11 Communication via Electronic Mail, Gulf.mex Bulletin Board.

Hamilton, P. (1990). Deep Currents in the Gulf of Mexico, Journal of Physical Oceanography 20: 1087-1104.

Hofmann, E.E. and S.J. Worley (1986). An Investigation of the Circulation of the Gulf of Mexico, Journal of Geophysical Research 91 (C12): 14,221-14,236.

Meserve, J.M. (1974). U.S. Navy Marine Climatic Atlas of the World, Volume 1, North Atlantic Ocean, NAVAIR 50-1C-528, U.S. Dept. of Commerce, National Climatic Center, 371 pp.

Naval Oceanography Command Detachment (1986). U.S. Navy Climatic Study of the Caribbean Sea and Gulf of Mexico, Volume 4, Gulf of Mexico and Gulf of Tehuantepec, NAVAIR 50-1C-546, prepared for Commander, Naval Oceanography Command, 198 pp.

Neumann, C.J., B.R. Jarvinen, A.C. Pike, and J.D. Elms (1987). Tropical Cyclones of the North Atlantic Ocean, 1871-1986, NOAA Historical Climatology Series 6-2, U.S. Dept. of Commerce, National Oceanic and Atmospheric Administration, 186 pp.

Nowlin, W.D., Jr. and H.J. McLellan (1967). A Characterization of the Gulf of Mexico Waters in Winter, Journal of Marine Research 25(1): 29-59.

Rocker, K., Jr. (1985). Handbook for Marine Geotechnical Engineering, Naval Civil Engineering Laboratory, Port Hueneme, CA, pp. 2-1 - 4-29.

Science Applications International Corporation (SAIC) (1989). Gulf of Mexico Physical Oceanography Program Final Report: Year 5, prepared for Dept. of the Interior, Minerals Management Service, OCS Study MMS 89-0068, 333 pp.

Smith, D.C., IV (1986). A Numerical Study of Loop Current Eddy Interaction with Topography in the Western Gulf of Mexico, Journal of Physical Oceanography 16: 1260-1272.

Sturges, W. and J.C. Evans (1983). On the Variability of the Loop Current in the Gulf of Mexico, Journal of Marine Research 41: 639-653.

U.S. Dept. of the Interior, Minerals Management Services (MMS) (1987). Gulf of Mexico Physical Oceanography Program Final Report Year 4, Volume II: Technical Report, OCS Study MMS 87-0007, prepared by Science Applications International Corporation, 226 p. plus appendices.

U.S. Dept. of the Interior, Minerals Management Services (MMS) (1987). Gulf of Mexico Physical Oceanography Program Final Report Years 1 and 2, Volume II: Technical Report, OCS Study MMS 85-0094, prepared by Science Applications International Corporation, 378 p.

U.S. Dept. of the Interior, Minerals Management Service (MMS) (1984). Final Environmental Impact Statement Proposed Oil and Gas Lease Sales 94, 98, and 102, OCS EIS MMS 84-0057, prepared by the Gulf of Mexico OCS Region, 752 p. plus visuals.

U.S. Dept. of the Interior, Minerals Management Service (MMS) (1983). Regional Environmental Assessment, Gulf of Mexico, Pipeline Activities, MMS Gulf of Mexico OCS Region, 175 pp.

Vukovich, F.M. (1988). On the Formation of Elongated Cold Perturbations off the Dry Tortugas, Journal of Physical Oceanography 18: 1051-1059.

Wallcroft, A.J. (1984). Gulf of Mexico Circulation Modeling Study, Annual Progress Report, OCS Study MMS 85-0025, 106 p.

Distribution List

Edward Barrett
Code 64
Naval Ocean Systems Center
San Diego, CA 92152

Dr. Henri Berteaux
Woods Hole Oceanographic Institution
Woods Hole, MA 02543

Dr. Newell Booth
Code 705(T)
Naval Ocean Systems Center
San Diego, CA 92152-5000

Commander
Naval Ocean Systems Center
Code 64H
San Diego, CA 92152-5000

Dr. Richard Doolittle
Code 230
Office of Naval Technology
800 N. Quincy Street
Arlington, VA 22217-5000

Dr. Fred Fisher
Marine Physics Laboratory
Scripps Institution of Oceanography
San Diego, CA 92152

Dr. Mark Grosenbaugh
Woods Hole Oceanographic Institution
Woods Hole, MA 02543

Robert Hearn
Code 702
Naval Ocean Systems Center
San Diego, CA 92152

CDR W. Hickman
Code 230
Office of Naval Technology
800 N. Quincy St.
Arlington, VA 22217-5000

Dr. William Hodgkiss
Marine Physical Laboratory
Scripps Institution of Oceanography
San Diego, CA 92152

Bill Macha
Code 942
Naval Ocean Systems Center
San Diego, CA 92152

Dr. Jim Mercer
Applied Physics Laboratory
U of Washington
1013 NE 40th Street
Seattle, WA 98107

Jim Reese
Code 715
Naval Ocean Systems Center
San Diego, CA 92152-5000

David Shields
Code L40P
Naval Civil Engineering Laboratory
Port Hueneme, CA 93043

Richard Swenson
Neptune Technologies, Inc
100 Airport Road
Picayune, MS 39466

Robert Taylor
Code L42
Naval Civil Engineering Laboratory
Port Hueneme, CA 93043

Jeff Wilson
Code L43P4
Naval Civil Engineering Laboratory
Port Hueneme, CA 93043

Dr. Peter Worcester
Scripps Institution of Oceanography, A-013
University of California at San Diego
La Jolla, CA 92093

NOARL Code 125L (10)
Code 125P
Code 200
Code 253 M. Fagot (3)
Code 300
Code 330 A.W. Green
Code 331 R. Hollman
Code 331 J. Boyd (10)

REPORT DOCUMENTATION PAGE

Form Approved
OBM No. 0704-0188

1. Agency Use Only *(Leave blank).*	2. Report Date.	3. Report Type and Dates Covered.
	October 1990	Final

4. Title and Subtitle.
Environmental Conditions in the Gulf of Mexico During November - December

5. Funding Numbers.

Program Element No.	62435N
Project No.	03536
Task No	J0D
Accession No.	DN258033

6. Author(s).
J. D. Boyd, L. A. Jugan*, M. A. Rich* and B. J. Roser*

7. Performing Organization Names(s) and Address(es).
Naval Oceanographic and Atmospheric Research Laboratory
Ocean Science Directorate
Stennis Space Center, Mississippi 39529-5004

8. Performing Organization Report Number.
NOARL Technical Note 83

9. Sponsoring/Monitoring Agency Name(s) and Address(es).
Office of Naval Technology
800 N. Quincy Street
Arlington, VA 22217-5000

10. Sponsoring/Monitoring Agency Report Number.
NOARL Technical Note 83

11. Supplementary Notes.
*Planning Systems Incorporated
Slidell, Louisiana

12a. Distribution/Availability Statement.
Approved for public release; distribution is unlimited.

12b. Distribution Code.

13. Abstract *(Maximum 200 words).*

Environmental information for the Gulf of Mexico was analyzed in support of an upcoming experiment. Available oceanographic, meteorological, and geological properties of the Gulf, with specific emphasis on the area between 24-29°N and 90-95°W, are summarized for the November-December time frame.

14. Subject Terms.
(U) Physical Oceanography, (U) Marine Engineering, (U) Marine Geology

15. Number of Pages.
44

16. Price Code.

17. Security Classification of Report.	18. Security Classification of This Page.	19. Security Classification of Abstract.	20. Limitation of Abstract.
Unclassified	Unclassified	Unclassified	SAR